# The influence of irradiance and interspecific differences on $\delta^{11}$ B, $\delta^{13}$ C

# 2 and elemental ratios in four coralline algae complexes from Aotearoa,

# New Zealand

4

3

5 Maxence Guillermic<sup>1</sup>, Erik C. Krieger<sup>2,3</sup>, Joyce Goh<sup>1</sup>, Christopher E. Cornwall<sup>2</sup>, Robert A. Eagle<sup>1</sup>

6

- 7 Department of Atmospheric and Oceanic Sciences, Institute of the Environment and Sustainability, Center for Diverse
- 8 Leadership in Science, University of California Los Angeles, CA 90095
- 9 <sup>2</sup>School of Biological Sciences, Victoria University of Wellington, Wellington, New Zealand
- <sup>3</sup>Red Sea Research Center, King Abdullah University of Science and Technology, Thuwal, Saudi Arabia

11 12

- Correspondence to: Maxence Guillermic (maxence.guillermic@gmail.com) and Robert Eagle (robeagle@g.ucla.edu)
- 13 **Abstract.** Coralline algae are a cosmopolitan group of important foundational species. The calcium carbonate they produce is 14 increasingly being used as paleoenvironmental archives, as well as used to trace physiological responses of these important 15 macroalgae to environmental change. In this context, evaluating the effect of oceanic change and photo-physiological 16 parameters on geochemical proxies is critical, as such gaps may lead to erroneous paleoenvironmental reconstructions, 17 misattributed drivers of calcification responses, and ultimately compromise conservation strategies. Here we address the 18 impact of light (irradiance) on four species complexes of coralline red algae including two morphologies; geniculate (branching) and non-geniculate (encrusting). The four complexes up-regulated their  $\delta^{11}B$  derived pH<sub>CF</sub> relative to seawater by 19 20 0.6 to 0.8 pH unit.  $\delta^{11}$ B was not measurably affected by varying irradiance despite evidence of increasing photosynthesis. All 21 complexes were able to maintain and elevate their pH<sub>CF</sub> relative to seawater for all treatments. Non-geniculate and geniculate complexes had distinct geochemical signatures of  $\delta^{11}$ B,  $\delta^{13}$ C<sub>mineral</sub> and trace elements. These differences in geochemical 22 23 signatures indicate a variety of calcification mechanisms exist within coralline algae. We propose that different sources of 24 dissolved inorganic carbon (DIC) are necessary to explain the observed  $\delta^{13}C_{\text{mineral}}$ . As geniculate species have higher 25 photosynthetic activity (i.e. gross photosynthesis), the DIC sources allocated to calcification might be limited due to greater 26 CO<sub>2</sub> drawdown. This is supported by B/Ca and U/Ca ratios suggesting modulation of carbonate chemistry and especially lower 27 DIC<sub>CF</sub> in geniculate relative to non-geniculate complexes. DIC sources might come from direct CO<sub>2</sub> diffusion or better 28 recycling of metabolic CO<sub>2</sub> which would explain the depleted  $\delta^{13}$ C<sub>mineral</sub>. This strategy likely arises from the different energy

needs of the organisms, with non-geniculate using relatively more energy to support calcification. We suggest the different calcification mechanisms between morphologies are linked to different interactions between photosynthesis and carbon allocation. While photosynthesis can provide energy to geniculate complexes to maintain their metabolic needs, their calcification may be limited by DIC. In contrast, non-geniculate forms may benefit from more limited DIC drawdown due to lower photosynthetic activity, therefore maintaining higher internal DIC concentrations ultimately supporting faster calcification.

#### 1 Introduction

Coralline algae are widespread foundational species found around the globe, and in some locations their calcium carbonate forms maerl or rhodolith beds which are the dominant benthic substrate of the area (Steneck et al., 1986). In other cases they can form ecologically and structurally significant contributions to other benthic environments, for example in tropical coral reefs (Cornwall et al., 2023) and within kelp forests (Connell, 2003b, Irving et al., 2004). Coralline red algae show two main morpho-functional groups, geniculate and non-geniculate. Geniculate corallines have non calcified joints that connect the calcified intergenicula to allow for higher thallus flexibility, distinct morphological traits allow them to grow in various habitats and to cope with a wide range of environments (Noisette et al., 2013; McCoy and Kamenos, 2015). As with other marine calcifiers, they are potentially threatened by ocean warming and acidification, evidence suggests they have plasticity and resilience to some of these climate change stressors (Anthony et al., 2008; Martin et al., 2013a; Cornwall et al., 2019).

Coralline algae are important in the field of paleoenvironmental reconstruction, particularly as they may grow in cooler regions such as the Arctic, where other commonly used archives such as mounding corals or foraminifera are not available (e.g., Halfar et al., 2000; Kamenos et al., 2008; Anagnostou et al., 2019). To increase the reliability of coralline algae for paleoclimate reconstruction, a better understanding of biomineralization mechanisms and how those mechanisms are impacted by environmental drivers is needed. This is critical as erroneous interpretation of proxies can undermine confidence in long-term environmental records, drivers of calcification and compromise forecasts that inform marine policy and conservation strategies.

Boron isotopes have been developed in carbonate as a proxy of pH in the fluid that it is precipitated within. The sensitivity of the  $\delta^{11}$ B proxy to pH is based on the predominant incorporation of borate ion in the carbonate structure (Hemming and Hanson, 1992). Carbonate skeletal  $\delta^{11}$ B has been used to explore pH of the calcifying fluid (pH<sub>CF</sub>) and carbonate chemistry regulation in coralline algae in response to environmental change such as ocean acidification (Cornwall et al., 2017, 2020; Donald et al., 2017; Sutton et al., 2018; Liu et al., 2020), with evidence suggesting that the calcifying environment of coralline algae have pH elevated with respect to seawater (Cornwall et al., 2017; Donald et al., 2017; Sutton et al., 2018; Liu et al., 2020) as has been observed in scleractinian corals (McCulloch et al., 2017; Eagle et al., 2022).

The most significant body of work on geochemical tracers of internal pH and carbonate chemistry regulation has primarily focused on symbiont bearing surface corals indicating that the photophysiology of the symbiont may influence the chemical regulation of calcification. For example, regulation of the pH of the calcifying medium within the calicoblastic epithelium is known to show day-night cycles (Al-Horani et al., 2003; Guillermic et al., 2021; Cameron et al., 2022). Corals that lose symbionts during temperature stress, may also exhibit a deregulation of the calcification fluid chemistry and anomalous skeletal geochemical signatures (e.g., D'Olivio et al., 2017; Guillermic et al., 2021; Cameron et al., 2022). Conversely, heat resilient corals may not undergo this process (Eagle et al., 2022). Varying light levels can also influence coral skeletal geochemistry in controlled culture experiments (Dissard et al., 2012; Juillet-Leclerc et al., 2014). Limited research has been carried out on coralline algae, and although irradiance can impact pH<sub>CF</sub> of coralline algae (Comeau et al., 2019), much more research is required.

Carbon isotopes of the mineral ( $\delta^{13}C_{mineral}$ ) and the tissues ( $\delta^{13}C_{tissue}$ ) can reflect photosynthesis and respiration (McConnaughey et al., 1997), where direct HCO<sub>3</sub><sup>-</sup> uptake from seawater enriches  $\delta^{13}C$  while recycling of respired CO<sub>2</sub> can decrease  $\delta^{13}C$  of the DIC pool. Additionally, increased uptake of diffusive CO<sub>2</sub> (from seawater or metabolic) can result in depletion in <sup>13</sup>C. Ultimately, the  $\delta^{13}C_{mineral}$  reflects the relative abundance of photosynthetic HCO<sub>3</sub><sup>-</sup> uptake relative to respiration processes or passive CO<sub>2</sub> diffusion from seawater. The  $\delta^{13}C_{tissue}$  represents the source of DIC and kinetic fractionation by RUBISCO during photosynthesis, RUBISCO enzyme preferentially fixing <sup>12</sup>C leading to  $\delta^{13}C_{tissue}$  being depleted relative to  $\delta^{13}C_{mineral}$ .

Coralline algae are photosynthetic organisms that inhabit various habitats where light fluctuates greatly. Increasing irradiance generally enhances calcification of coralline red algae (Goreau, 1963; Borowitzka 1981; Borowitzka and Larkum 1987; Martin et al. 2013a; Korbee et al., 2014; Egilsdottir et al., 2016; Krieger et al. 2023). Increasing irradiance on low-light adapted species can result in photoinhibition (Kain, 1987; Sagert et al., 1997; Kühl et al., 2001; Roberts et al., 2002; Martin et al., 2013b). In contrast, coralline algae in polar regions can continue calcifying at reduced rates even under prolonged low-light conditions associated with seasonal cycles or sea ice cover (Williams et al., 2018; Gould et al., 2022). These latitudinal (e.g. tropical, temperate or polar environments) and climate-driven differences in light adaptation and calcification mechanisms can contribute to the variability reported across studies. Although light clearly affects calcification, the mechanistic links between irradiance, photophysiology, and calcification is not fully understood.

A direct link between photosynthesis and the calcification space is hypothesised, as calcification is active in the meristematic region where there is a high concentration of chloroplasts. Photosynthesis has multiple ways in which it could promote calcification: 1) increase pH within the diffusive boundary layer surrounding the cells during the day via CO<sub>2</sub> removal, 2) provide the cell wall polysaccharides and proteins, and 3) provide energy to the cell formation and calcifying medium carbonate chemistry regulation (McCoy et al. 2023). Environmental parameters influencing irradiance in natural settings can change population communities and functionality of the ecosystem thus a good understanding of the mechanisms influencing calcification (including light) is needed to foresee changes due to future environmental challenges.

Krieger et al. (2023) explored the physiology and photophysiology of low-light coralline algae complexes *Phymatolithopsis repanda, Pneophyllum* spp. *Corallina* spp., and *Arthrocardia* spp. cultured under different irradiances and proposed that light-enhanced calcification is the result of an elevated diffusion boundary layer pH which raises calcifying fluid pH<sub>CF</sub> and that [Ca]<sub>CF</sub> could be the limiting parameters for fast growing species as also observed in Comeau et al. (2019). To further test Krieger et al's and Comeau et al's hypothesis we investigated calcification differences between faster and slower growing coralline algae complexes using geochemical tracers. Here we explore the underlying mechanisms behind interspecific differences and the effect of changing irradiance on coralline red algae complex calcification using geochemical tracers, namely the boron, carbon and oxygen isotopic compositions ( $\delta^{11}$ B,  $\delta^{13}$ C) as well as minor elemental compositions (Mg/Ca, Sr/Ca, Li/Ca, B/Ca, Ba/Ca).

#### 2 Materials and Method

#### 2.1 Specimens and culture experiment

Culturing experiments on non-geniculate coralline algae of different morphology ("thick" = Phymatolithopsis repanda; "smooth" = Pneophyllum spp.) as well as two groups of geniculate corallines ("fine" = Corallina spp.; and "robust" = Arthrocardia spp.) were described in a previous study (Krieger et al., 2023) an shown in Fig. 1. To briefly summarize this work, specimens were collected by scuba divers at depths between 1 and 2 m from two field sites located in Te Moana-o-Raukawa Cook Strait, Te Whanganui a Tara Wellington, Aotearoa New Zealand. Taxonomic and DNA-based identifications are described in Krieger et al. (2023). Samples can form a complex containing multiple species with a dominant presence of one species (Krieger et al., 2023). Those complexes present characteristic physiological and geochemical responses. For clarity, non-geniculate complexes will be referred to as Phymatolithopsis complex, Pneophyllum complex white geniculate complexes will be referred to as Corallina/Arthrocardia fine, Corallina/Arthrocardia robust. Specifically, Phymatolithopsis complex consists of Phymatolithopsis repanda (Hapalidiales ZT 75% and Hapalidiales sp. D 25%). Pneophyllum complex consists of 75% Pneophyllum sp. F and 25% Corallinales sp. E. Corallina/Arthrocardia morphologies fine and robust consists of 75% Corallina sp. and 25% Arthrocardia sp.

The original culture experiment was conducted over the 2019 summer and autumn (17th February to 19th May) in the facilities of the Victoria University of Wellington Coastal Ecology Laboratory. A detailed description of the original tank experiment can be found in Krieger et al. (2023) but we will briefly outline the most important information relevant for the present study here. The study organisms were exposed for 85 days to four different light levels (daily doses 0.6, 1.2, 1.8, 2.3 mol photons m<sup>-2</sup> d<sup>-1</sup>; noon peak irradiance 20, 40, 60, 80 µmol photons m<sup>-2</sup> s<sup>-1</sup>) that represent naturally occurring subcanopy irradiances at the collection sites. The chosen values approximate minimum summer irradiances, which are ecologically relevant as such low-light conditions often dominate under the canopy. Each irradiance level (i.e., treatment) was replicated twelve times on the tank level. The twelve tanks from each treatment were distributed over eight water baths with

each bath housing between one to two tanks from each treatment. Eight header tanks each supplied six different experimental tanks which were equally distributed between two neighboring water baths with 150 mL min<sup>-1</sup> of fresh filtered (10  $\mu$ m) seawater each. Water bath and header tank identity of each experimental tank was later used during the statistical analysis to remove sample interdependence. Light was provided by LED panels which simulated a natural diel light cycle and mimicked a typical temperate coastal underwater light spectrum. Temperature control was achieved by using submersible heaters and aquarium chillers with the difference in mean treatment temperature between treatments was not higher than 0.1 °C (highest  $16.45 \pm 0.1$  SE and lowest  $16.36 \pm 0.1$  SE). Seawater carbonate chemistry was monitored frequently through the measurement of tank pH<sub>T</sub> and total alkalinity. Mean treatment total alkalinity was within 4  $\mu$ mol kg<sup>-1</sup> (highest  $2279.77 \pm 3.41$  SE and lowest  $2275.11 \pm 4.88$ SE) while pH<sub>T</sub> was within 0.1 units (highest  $8.02 \pm 0.01$  SE and lowest  $8.01 \pm 0.01$  SE). Samples were stained with alizarin red and only material above the stain line was sampled to ensure sampling the new growth.

#### 2.2 Specimens and culture experiment

Photosynthetic (Chl a content, Fv/Fm, ETRmax, gross photosynthesis) and physiological (net calcification) parameters as well as tissue  $\delta^{13}$ C were originally published in Krieger et al. (2023) and are also presented in Table S1. Physiological data against irradiance are also presented in Fig. 2.

#### 2.3 Carbonate geochemistry

Methods used in this study were previously described in Guillermic et al. (2020, 2021, 2022) and Eagle et al. (2022). Briefly, powdered calcium carbonate samples were organically cleaned using a solution of 0.2 % hydrogen peroxide. Samples were dissolved in 1 N HCl and purified for boron isotopes through microdistillation (Gaillardet et al., 2001, Wang et al., 2008). Boron isotopic measurements were carried out on a Thermo Scientific® Neptune MC-ICP-MS at the Pôle Spectrométrie Océan (PSO), Plouzané and at the Dornsife PLASMA Facility of the University of Southern California, Los Angeles.

Elemental ratios were measured on a Thermo Fisher Scientific Element XR HR-ICP-MS at the PSO, Ifremer (Plouzané, France) after [Ca] analyses on an ICP-AES Ultima 2 HORIBA at the PSO (Plouzané, France). Data quality and external reproducibility were monitored by repeated measurement of JCp-1 (Gutjarh et al., 2021), NIST RM 8301 (Stewart et al., 2020) and filtered seawater for both boron isotopes measurements and trace elements.  $\delta^{11}$ B measured for NIST 8301 coral was 24.26  $\pm$  0.22 ‰, 2 SE, n=19 (published value is 24.17  $\pm$  0.07 ‰, 2 SE, n=7, Stewart et al., 2020),  $\delta^{11}$ B of JCp-1 was 24.51 $\pm$  0.14 ‰, 2 SE, n=12 (published value is 24.36  $\pm$  0.14 ‰, 2 SE, n=10, Gutjarh et al., 2021) and  $\delta^{11}$ B measured for a filtered seawater was 39.53  $\pm$  0.12 ‰, 2 SE, n=2 (published value is 39.61  $\pm$  0.04 ‰, 2 SE, n=28, Foster et al., 2010).

Analyses of carbonate skeletal  $\delta^{13}$ C and  $\delta^{18}$ O were carried out on a Matt 253 (Kiel IV carbonates, dual Inlet) mass spectrometer at the stable isotope facility of Pôle spectrométrie Océan (PSO, Plouzané, France). Results were calibrated to the Vienna Pee Dee Belemnite (V-PDB) scale and referenced to the international standard NBS19.

Geochemical data analyzed in this study are presented in Table S1 and Fig. 3.

#### 2.4 pH<sub>CF</sub> calculations

The pH<sub>CF</sub> was calculated from measurements of coral skeletal  $\delta^{11}B$  following Hemming and Hanson (1992) and equation from Zeebe and Galdrow, (2001):

$$pH_{CF} = pK_B^* - \log\left(-\frac{\delta^{11}B_{seawater} - \delta^{11}B_c}{\delta^{11}B_{seawater} - \alpha^*\delta^{11}B_c - \epsilon}\right)$$
eq. 1

with pK<sub>B</sub>\*(T,S) representing the dissociation constant, temperature of 16.4 °C and salinity of 35 psu.  $\delta^{11}$ B<sub>seawater</sub> is representing the boron isotopic composition of seawater (Foster et al., 2010),  $\delta^{11}$ B<sub>c</sub> representing the boron isotopic composition of the mineral (e.g. high-Mg calcite of coralline red algae), and  $\alpha$  representing the fractionation factor and  $\epsilon$  representing the boron isotopic fractionation between boric acid and borate ion (27.2 %, Klochko et al., 2006).

#### 2.5 Statistical analyses

Linear and quadratic models were compared using Akaike information criterion (AIC) to determine which model best described the data (Figs. S1, S2, Tables S2, S3). Only significant lines were plotted for the regressions that had a significant p-value (for linear fit) or R<sup>2</sup> (for quadratic fit) (Figs. S1, S2). Statistical tests were performed between the geochemical data and matching photophysiological data from Krieger et al. (2023).

Normality of the data was assessed and data transformed using R to normalize the entire dataset (by variable) using Box-Cox transformation and then subsequently tested the normality of the data set using the Shapiro Normality Test and Q-Q plot.

ANOVA tests in R were used to evaluate the effect of irradiance and test differences between species. ANOVA tests that had a significant p-value were then further analyzed using the TukeyHSD Multiple Comparisons of Means test at a family-wise confidence level of 95%. Results are presented in Tables S4, S5, S6 and S7.

Correlation matrices are a statistical method that evaluates the correlation between multiple parameters and allows representation of complex datasets. Correlation matrices were performed using R for each complex and are presented in Figs. S4 and S5. These correlation matrices were used to visually present the data and support interpretation from regression models and other statistical methods used in this paper.

Principal component analysis (PCA) was made using Graphpad Prism (version 10.2.3 for Windows GraphPad Software, Boston, Massachusetts USA, "www.graphpad.com") for all trace elements and physiological parameters. Relevant physiological parameters were selected, ETRmax and  $\delta^{13}C_{\text{organic}}$  given the reduced amount of data (Fig. 4).

The averages of photophysiological parameters presented in Figs. 2, 4, and 6 are derived from the full dataset provided in the supplemental information of Krieger et al. (2023). Regression analyses and other statistical tests were conducted on a subset of photophysiological samples for which geochemical analyses were available (Table S1). Individual paired data and averages are shown in the cross-plots in Figs. 5 and 7 in order to display maximum information on the data.

#### 3 Results

#### 3.1 Net calcification and changing irradiance

No significant relationship was observed between net calcification and irradiance (p > 0.05, ANOVA) in our subset of data. Differences in net calcification were only significant between complexes (p < 0.05, ANOVA for irradiance 0.6, 1.8, 2.3). However, Krieger et al. (2023) presented two significant relationships, one non-linear for *Corallina* and one non-linear for *Spongites* when the full dataset was taken into account.

#### 3.2 $\delta^{13}$ C<sub>mineral</sub> and $\delta^{13}$ C<sub>tissue</sub>

The geniculate and non-geniculate complexes present different absolute values of  $\delta^{13}C_{mineral}$  and responses with increasing irradiance. Relatively lower  $\delta^{13}C_{mineral}$  values (~ -5.5 %) are observed for geniculate *Corallina/Arthrocardia* fine and *Corallina/Arthrocardia* robust; non-geniculate *Phymatolithopsis* complex and *Pneophyllum* complex have relatively enriched  $\delta^{13}C_{mineral}$  signatures (~ -2.5 %). Significant differences in  $\delta^{13}C_{mineral}$  between species were observed for all irradiances (Table S6).

ANOVA results indicate a significant effect of irradiance on  $\delta^{13}C_{mineral}$  of the non-geniculate species (*Phymatolithopsis complex* and *Pneophyllum complex*) (p=0.01 and p=0.009, Table S4). These two complexes exhibit a significant linear increase in  $\delta^{13}C_{mineral}$  with increasing irradiance levels (p=0.010 and p=0.003, respectively, Table S2). The geniculate *Corallina/Arthrocardia* fine is showing a non-linear (R<sup>2</sup>=0.45) significant increase in  $\delta^{13}C_{mineral}$  while *Corallina/Arthrocardia robust* is having a relatively stable  $\delta^{13}C_{mineral}$  signature for the different treatments (p=0.948).

 $\delta^{13}C_{tissue}$  data were already presented in Krieger et al. (2023). In our subset of samples, ANOVA supports a significant effect of irradiances for non-geniculate *Phymatolithopsis* complex and *Pneophyllum* complex (p=0.009, p=0.011). Values of  $\delta^{13}C_{tissue}$  are linearly increasing with higher irradiances for *Phymatolithopsis* complex (p=0.001), and a significant non-linear relationship is observed for *Pneophyllum* complex (R<sup>2</sup>=0.58). ANOVA also supports significant differences between species (Table S6).

 $\delta^{13}C_{mineral}$  are enriched in comparison to  $\delta^{13}C_{tissue}$  by 9 to 22 ‰. Significant positive linear relationships between  $\delta^{13}C_{mineral}$  and  $\delta^{13}C_{tissue}$  were observed for the non-geniculate *Pneophyllum* complex and *Phymatolithopsis* complex (p=0.025, p=0.003), but not for the geniculate *Corallina/Arthrocardia* fine and *Corallina/Arthrocardia* robust, Fig. 5A.

There is an increase in  $\delta^{13}C_{mineral}$  with increasing net calcification across all complexes (p<0.001; Fig. 5C). Some differences to note are that the geniculate *Corallina/Arthrocardia* robust and *Corallina/Arthrocardia* fine have the lightest  $\delta^{13}C_{mineral}$  in line with observed lower net calcification. The non-geniculate complexes have higher net calcification and higher  $\delta^{13}C_{mineral}$ , implying different sensitivities of net calcification to irradiance between complexes and difference between non-geniculate and geniculate complexes.

#### 3.3 $\delta^{11}$ B

Enriched  $\delta^{11}B$  values are observed for the geniculate *Corallina/Arthrocardia* robust (~26.4 ‰) and *Corallina/Arthrocardia* fine (~27.4 ‰), compared to the non-geniculate *Pneophyllum* complex (~24.5‰) and *Phymatolithopsis* complex (~25.4 ‰). The differences between complexes are significant at irradiance 0.6, 1.8 and 2.3 (ANOVA p=0.008, p=0.001, p=0.006, respectively, Table S6).

No significant linear or non-linear regression was observed between  $\delta^{11}B$  and irradiance (Tables S3 and S4).  $\delta^{11}B$  differences were observed between species (ANOVA significant for most irradiances, Tables S3 and S4). T-tests show no significant differences between *Corallina/Arthrocardia* fine and *Corallina/Arthrocardia* robust (geniculate) or *Phymatolithopsis* complex and *Pneophyllum* complex (non-geniculate) but do show significant differences between geniculate and non-geniculate species.

Crossplot of  $\delta^{13}C_{mineral}$  and  $\delta^{11}B$  does show significant negative linear relationships across all complexes (p<0.0001), not significant at the complex level (Fig. 5B). There is a clear distinction between non-geniculate and geniculate species. Corallina/Arthrocardia robust and Corallina/Arthrocardia fine show depleted  $\delta^{13}C$  and high  $\delta^{11}B$  while Pneophyllum complex show enriched  $\delta^{13}C$  and lower  $\delta^{11}B$  (significant ANOVA).

 $\delta^{13}$ C and  $\delta^{11}$ B compared to net calcification and gross photosynthesis (Figs. 5C, 5D, 5E and 5F) do not present any significant relationships. We note that higher  $\delta^{11}$ B and lower  $\delta^{13}$ C<sub>mineral</sub> coincides with higher gross photosynthesis and lower net calcification in the geniculate species while the opposite is true for non-geniculate species (Fig. 5).

#### 3.4 Trace elements

Li/Ca, B/Ca, Mg/Ca, Sr/Ca, Ba/Ca, U/Ca were analyzed in this study. Mg/Ca was the most impacted by irradiance between complexes, while Li/Ca was significantly impacted in *Pneophyllum* complex (p<0.001, ANOVA, Table S4) and Ba/Ca in *Corallina/Arthrocardia* robust (p<0.04, ANOVA). Most elements presented significant differences between complexes, including B/Ca, Li/Ca, Mg/Ca, Sr/Ca (ANOVA, Table S6).

Mg/Ca observed are significantly different between species at irradiance 0.6, 1.8 and 2.4 (p=0.047, p=0.03 and p<0.001, ANOVA). Significant quadratic relationships between Mg/Ca and irradiance are observed for *Pneophyllum* complex and *Phymatolithopsis* complex ( $R^2$ =0.51,  $R^2$ =0.48) while a positive linear relationship is observed for *Corallina/Arthrocardia* fine (p=0.002) are best fit according to AIC analyses (Table S2, Fig.

S1). There is a significant impact of irradiance on Mg/Ca for *Corallina*, *Pneophyllum* complex and *Phymatolithopsis* complex (p=0.03, p=0.003 and p=0.04, ANOVA, Fig. S1, Table S2, S4).

Significant positive relationships are observed between B/Ca and irradiance, quadratic for *Pneophyllum* complex and linear for *Phymatolithopsis* complex (R<sup>2</sup>=0.40, p=0.02 respectively) but not for other complexes. Based on TukeyHSD Multiple Comparisons of Means (see method section) B/Ca was significantly different for the species for the three irradiance treatments, 0.6, 1.2 and 1.8 (p=0.006, p=0.02 and p=0.0003 respectively, Fig. S1, Tables S2, S6).

#### 3.5 Other physiological parameters

Maximum electron transport rate (ETR max) is an important photophysiological parameter indicative of photosynthetic capacity. ETR max is directly correlated to gross photosynthesis (μg O<sub>2</sub>.cm<sup>-2</sup>.h<sup>-1</sup>) making it a key parameter to study the impact of changing irradiance in coralline red algae. In our subset of samples ETR max had significant positive linear relationships with irradiance for *Corallina/Arthrocardia* robust, *Corallina/Arthrocardia* fine and *Pneophyllum* complex (p= 0.035, p=0.0023, p=0.0238 respectively), Table S3, Fig. S2. Chl *a*, ETRmax and Fv/Fm were significantly different between species at different irradiance levels based on ANOVA (Table S6).

Significant differences between non-geniculate and geniculate complexes were observed in the photophysiological parameters. Net calcification was lower in geniculate complexes than in non-geniculate complexes (t-test, p<0.001). Gross photosynthesis was higher in geniculate complexes than in the non-geniculate ones (t-test, p<0.001).

#### 3.6 Principal component analysis (PCA) and correlation matrices.

Principal component analysis (PCA) was performed for the geochemical and physiological data. The isotopic and trace element measurements were dissociated for better clarity of the figures. Vectors present a positive relationship between ETRmax and irradiance, a negative relationship between net calcification and  $\delta^{11}B$ , positive relationships between net calcification and  $\delta^{13}C_{mineral}$  and between  $\delta^{11}B$  and Fv/Fm. (Fig. 4 and S3).

In both cases, geniculate and non-geniculate species cluster together. Non-geniculate complexes (*Pneophyllum* complex and *Phymatolithopsis* complex) show higher net calcification, higher  $\delta^{13}C_{\text{mineral}}$  and lower  $\delta^{11}B$ . Geniculate complexes *Corallina/Arthrocardia* robust and *Corallina/Arthrocardia* fine on the contrary show lower net calcification, lower  $\delta^{13}C_{\text{mineral}}$  and higher  $\delta^{11}B$ . The clustering is also observed with the trace elements. Geniculate complexes showing higher Li/Ca, Sr/Ca, Ba/Ca and U/Ca ratios than non-geniculate complexes (Fig. S3).

Complex-specific relationships between geochemical and physiological parameters are presented in the correlation matrices in Fig. 4.

#### 4 Discussion

## 4.1 Impact of irradiance is observed on $\delta^{13}C_{mineral}$ and $\delta^{13}C_{tissue}$

The positive relationships between  $\delta^{13}C_{mineral}$  and irradiance in three out of four complexes and the significant effect of irradiance on  $\delta^{13}C_{mineral}$  (i.e. *Corallina/Arthrocardia* fine and *Phymatolithopsis* complex) and  $\delta^{13}C_{tissue}$  (i.e. *Pneophyllum* complex and *Phymatolithopsis* complex) (p < 0.05, ANOVA), highlights: 1) that irradiance impacts the geochemical signatures of the mineral, 2) photosynthetically driven isotope fractionation increases with increasing irradiance based on  $\delta^{13}C_{mineral}$ . Those results are in line with photophysiological parameters measured (i.e. gross photosynthesis, ETRmax) showing increased

photosynthesis with irradiance at the complex level and supported by previous study that indicate  $\delta^{13}$ C changes with photosynthesis and respiration (McConnaughey et al., 1997).

Difference in sensitivities between  $\delta^{13}C_{mineral}$  and irradiance is observed between *Pneophyllum* complex and *Phymatolithopsis* complex indicating complex-specific responses to light. In the range of irradiances tested in this study, geniculate complexes are less sensitive to changes in irradiance (p=0.975) than the non-geniculate ones (p=0.0001), Fig 5A.

There are clear differences in  $\delta^{13}C_{mineral}$  signatures between non-geniculate and geniculate complexes. Non-geniculate complexes *Pneophyllum* complex and *Phymatolithopsis* complex are fast calcifiers that have enriched  $\delta^{13}C_{mineral}$  and a strong response to increased irradiance. Geniculate complexes *Corallina/Arthrocardia* fine and *Corallina/Arthrocardia* robust present lower net calcification and lower  $\delta^{13}C_{mineral}$ . Photosynthesis can increase the  $\delta^{13}C$  of the DIC pool available for calcification, the differences observed between morphotypes in  $\delta^{13}C_{mineral}$  and net calcification are then in line with a positive effect of photosynthesis on net calcification (Fig. 5C).

The geniculate complexes have higher gross photosynthesis here than the non-geniculate complexes, they also have lower  $\delta^{13}$ C<sub>mineral</sub> (Fig. 5E). The higher photosynthesis rate in geniculate versus non-geniculate has also been observed in the field (Nguyen et al., 2022). The discrepancy with  $\delta^{13}C_{\text{mineral}}$  (e.g. high photosynthesis/low c  $\delta^{13}C_{\text{mineral}}$ ) could be that the source of DIC used by geniculate species is depleted in <sup>13</sup>C, i.e., a greater use of recycled respiratory CO<sub>2</sub> and/or use of CO<sub>2</sub> via diffusion. The morphology of the geniculate algae represents a higher surface area-to-volume ratio and a thinner wall thickness; this might lead to greater passive transport of DIC to the site of calcification. On the contrary, the thick crust, and lower surface area to volume ratio of the non-geniculate species could lead to less passive diffusion as a source of DIC. Mao et al. (2024) established a carbon budget based on radiogenic-isotopes and highlighted that up to 40% of the carbon released during calcification was recycled internally. While carbon fixed during photosynthesis is not directly recycled into calcification, CO<sub>2</sub> released during respiration may contribute to calcification, potentially lowering  $\delta^{13}C_{mineral}$ . Because respiratory inputs are derived from photosynthetically fixed carbon,  $\delta^{13}$ C of the DIC pool available for calcification could be indirectly influenced by photosynthesis. We anticipate that this recycling will vary depending on morphologies and taxa and then impact  $\delta^{13}$ C. DIC uptake strategies can vary by coralline taxa (Bergstrom et al. 2020), especially CO<sub>2</sub> diffusion being more prevalent in basal taxa which highlight the diversity of carbon concentrating mechanisms in coralline algae. Our results show that the geochemical signatures of the mineral are impacted by changing irradiances thereby enabling the investigation of potential changes in pH<sub>CF</sub> constrained by boron isotopes.

### **4.2 Boron isotopes (δ**<sup>11</sup>**B)**

278

279

280281

282

283284

285

286

287288

289

290291

292

293

294

295

296

297

298299

300

301

302

303

304

305

306

307

308

309

310

There were significant differences between the  $\delta^{11}B$  of our four species. The range of  $\delta^{11}B$  seems consistent with sole incorporation of B(OH)<sub>4</sub><sup>-</sup> and realistic physiological modulation of pH<sub>CF</sub>. However, we note that NMR study from Cusack et al. (2015) observed the presence of trigonal boron (BO<sub>3</sub>) accounting for up to 30% of the total boron in *Lithothamnion glaciale*. The presence of BO<sub>3</sub> can also be due to the recoordination of BO<sub>4</sub> during the incorporation of boron within the crystal lattice (Klochko et al., 2009; Branson et al., 2015) which in that case would not impact the  $\delta^{11}B$  proxy. NMR studies on other species

of coralline red algae along with boron isotopic measurements are lacking to affirm that BO<sub>3</sub> does not contribute to a part of the signal measured. For example, more extreme  $\delta^{11}B$  data for *Neogoniolithon* were reported at (31-40) ‰ (Donald et al., 2017; Liu et al., 2020), even if BO<sub>3</sub> incorporation might not be the dominant driver, it could still contribute to the high values in that particular species/experiment (Donald et al., 2017; Liu et al., 2020). In our study, the range of  $\delta^{11}B$  reported (26 ± 3 ‰, 2 SD, n = 76, Fig. 3B) is consistent with the pH at the site of calcification (pH<sub>CF</sub>) and without further evidence of BO<sub>3</sub> incorporation and impact on the  $\delta^{11}B$ , the  $\delta^{11}B$  will be interpreted as a physiological signal in the following discussion.

#### 4.3 pH<sub>CF</sub> is up-regulated relative to seawater

The primary calcification happens in the interfilament space in coralline red algae, secondary calcification occurs within the cell walls (McCoy et al., 2023). It is thought that coralline red algae elevate their internal pH and modulate carbonate chemistry to promote calcification (Cornwall et al., 2017).  $\delta^{11}B$  is thought to record the pH at the site of calcification (pH<sub>CF</sub>). Boron based studies suggest that pH<sub>CF</sub> is upregulated relative to seawater supporting favorable saturation state and calcium carbonate precipitation, as observed in corals (McCulloch et al., 2017; Cornwall et al., 2017; Anagnostou et al., 2019; Comeau et al., 2019) and other marine organisms (Sutton et al., 2018; Liu et al. 2020). The capacity of coralline algae to maintain its pH<sub>CF</sub> has also been shown to be impacted by ocean acidification, as recorded by the boron isotope proxy of pH at the site of calcification (Cornwall et al., 2017; Comeau et al., 2019) and indirectly seawater pH (Anagnostou et al. 2019).

Upregulation of pH<sub>CF</sub> relative to seawater occurred here in the four complexes studied here with average values for *Corallina/Arthrocardia robust* and *Corallina/Arthrocardia fine* of 8.75 ± 0.21 (2 SD, n=19) and 8.81 ± 0.12 (2 SD, n=20), respectively and for *Pneophyllum complex* and *Phymatolithopsis complex* of 8.63 ± 0.20 (2 SD, n=18) and 8.68 ± 0.15 (2 SD, n=19), respectively (Fig. 6). The seawater pH (total scale) during the experiment was maintained to 8.02, meaning that internal pH for the four complexes was elevated relative to seawater by 0.6 to 0.8 pH unit. Complex-specific pH<sub>CF</sub> dynamics are observed: the geniculate species (*Arthrocardia/Corallina* fine and robust) show higher pH<sub>CF</sub> in comparison to the nongeniculate complexes (*Pneophyllum* complex and *Phymatolithopsis* complex). All pH<sub>CF</sub> values are in the range to sustain the saturation state based on boron-based study in other marine organisms (McCulloch et al., 2017; Sutton et al., 2018; Comeau et al., 2019; Liu et al., 2020; Guillermic et al., 2021 and others).

#### 4.4 pH<sub>CF</sub> is not affected by changing irradiance at the complex level

There was no effect of irradiance on pH<sub>CF</sub> for any of our species across all levels of irradiance. All complexes presented pH homeostasis responses at different irradiance levels and despite evidence of increased photosynthetic rates (Fig. 6). These results highlight complex-specific pH<sub>CF</sub>, the species are able to maintain an optimal pH<sub>CF</sub> demonstrating a good acclimation in the range of irradiance tested (0.6 to 2.3 mol photons m<sup>-2</sup> day<sup>-1</sup>). This is also in line with the complexes not showing significant changes in calcification with changing irradiances in our subset of samples (Table S3, Figs. 2, S2). For comparison, those  $\delta^{11}$ B-derived pH<sub>CF</sub> are higher than those measured via microelectrode in the light (8.15 - 8.30) in Arctic

corallines (Hoffman et al. 2018). This lack of response to changing irradiance may also result from photosynthesis-independent mechanisms (de Beer and Larkum, 2001; Hofmann et al., 2016, 2018) helping to maintain favorable proton gradients.

#### 4.5 Calcification space chemistry under changing irradiance

The relationship between calcification to photosynthesis is not fully understood in coralline red algae. While some studies report a positive effect of photosynthesis on calcification (Goreau 1963; Pentecost 1978; Comeau et al. 2014) others show non-linear responses to increase irradiance (Martin et al. 2013b; Egilsdottir et al. 2016) or photoinhibition that may affect calcification (Kain, 1987; Sagert et al., 1997; Kühl et al., 2001; Roberts et al., 2002; Martin et al., 2013b). The subset of data we used for this study did not show significant changes in net calcification which could result from a decoupling between photosynthesis and net calcification at specific irradiance conditions. Net calcification was maintained over the different treatments despite evidence of increasing photosynthesis. In other words, this suggests photosynthetic activity was sufficient even at the lowest irradiance to 1) provide a substantial provision of energy to the organism that can be allocated to active transports of ions and subsequent modulation of the calcification space chemistry, 2) sustain a proton gradient between the calcifying space and seawater. This gradient is maintained from elevation of pH surrounding the cells as result of photosynthetic rate and CO<sub>2</sub> drawdown (Hoffman et al., 2016; Cornwall et al., 2013, 2014, 2017) and by the presence of light-mediated proton pump that is independent from photosynthesis (Hoffman et al., 2016, 2018).

Increasing photosynthesis, however, can have other positive effects on the organism and calcification. For example photosynthesis may sustain calcification by providing the key constituents of organic molecules needed for cell wall formation which act as a template for mineral precipitation. Those organic molecules (like polysaccharides) can also have affinities with Ca which can increase locally the saturation state and promote precipitation of CaCO<sub>3</sub>. Overall, all complexes in this study acclimatized well to the different levels of irradiance, calcification was maintained but not improved. This can also result from other limiting parameters involved in the modulation of the saturation state at the site of calcification like DIC concentrating mechanisms and [Ca]<sub>CF</sub>.

Krieger et al. (2023) presented the full-width-half-maximum (FWHM) parameter which has been calibrated in aragonite as a proxy for saturation state (DeCarlo et al. 2017), no quantitative but qualitative analyses can be done when applied to calcite which is the case here. In our subset of data there was no significant change in FWHM in either of the complexes with increasing irradiances again highlighting a relatively stable saturation state across treatments, in line with  $pH_{CF}$  and calcification data.

B/Ca has been used as a proxy for [CO<sub>3</sub><sup>2-</sup>]<sub>CF</sub>, however this proxy has only been derived for aragonite so no quantitative estimate can be made here but can be used as a potential indication of changes in the carbonate parameters in the calcification space (McCulloch et al. 2017; DeCarlo et al. 2018b). No relationship is observed for the geniculate complexes of B/Ca with irradiance. Nevertheless, non-geniculate complexes present significant increase in B/Ca with increasing irradiances (parabolic for *Pneophyllum* complex, positive for *Phymatolithopsis* complex), which could highlight changes in the DIC pool (i.e., decreasing [CO<sub>3</sub><sup>2-</sup>]<sub>CF</sub> with increasing irradiance). Differences within the non-geniculate complexes are also observed with B/Ca

Phymatolithopsis complex < B/Ca $_{Pneophyllum}$  complex (i.e.,  $[CO_3^{2-}]_{CF}$  Phymatolithopsis complex >  $[CO_3^{2-}]_{CF}$  geniculate >  $[CO_3^{2-}]_{CF}$  phymatolithopsis complex >  $[CO_3^{2-}]_{CF}$  phyma

Mg/Ca is another parameter that could be used to infer the [Ca]<sub>CF</sub> following the approach of Krieger et al. (2023) with their %Mg. The rationale is that the Mg/Ca ratio of the mineral reflects the Mg/Ca ratio of the precipitating fluid, and that only [Ca] modulates this ratio due to its incorporation within the mineral. However, the presence of organics also influences [Ca] and [Mg], and there are additional controls on Mg incorporation like temperature (Williams et al., 2014) or change in precipitation rate (Gabitov et al., 2014) so a direct translation of Mg/Ca to [Ca]<sub>CF</sub> can be too simplistic. Nevertheless, a significant effect of irradiance on Mg/Ca is observed in three out of the four complexes. Different Mg/Ca responses can be observed, positive for *Corallina/Arthrocardia* fine, parabolic for *Pneophyllum* complex and threshold positive for *Phymatolithopsis* complex. Those responses are similar to the B/Ca responses for the non-geniculate complexes. This implies that when [Ca]<sub>CF</sub> decreases (i.e., Mg/Ca increases), [CO<sub>3</sub><sup>2-</sup>]<sub>CF</sub> also decreases (B/Ca increases) and that there is no compensation of changes in [Ca]<sub>CF</sub> by changing [CO<sub>3</sub><sup>2-</sup>]<sub>CF</sub>. The fact that variations have similar responses can also highlight the changes in [Ca]<sub>CF</sub> (i.e., driving changes in both Mg/Ca and B/Ca ratios).

#### 4.6 Differences of calcification space chemistry between geniculate and non-geniculate complexes

It is clear that the two morphologies have characteristic geochemical parameters and physiological responses (PCA and box plots, Figs. 4 and 8). We have shown that non-geniculate complexes have higher calcification (Krieger et al., 2023), higher  $\delta^{13}C_{minerals}$  lower gross photosynthesis and lower pH<sub>CF</sub> compared to geniculate species. From those results, differences between morphologies can be highlighted, 1) there is a decoupling between net calcification and gross photosynthesis, higher gross photosynthesis in the geniculate complexes does not translate in higher calcification relative to the non-geniculate complexes, 2)  $\delta^{13}C_{mineral}$  reflects different DIC source between the two morphologies,  $\delta^{13}C_{mineral}$  is not positively correlated with gross photosynthesis when comparing between morphotypes but it is at the complex level across experimental treatments, 3) despite a lack of relationships between pH<sub>CF</sub> and changing irradiance at the complex level, non-geniculate and geniculate complexes have two different photosynthetic regimes that could correlate with the pH<sub>CF</sub> observed, higher pH<sub>CF</sub> is observed along higher gross photosynthesis in geniculate complexes (Figs. 7, 8), 4) there is a decoupling between pH<sub>CF</sub> and net calcification, higher pH<sub>CF</sub> does not translate to higher net calcification (Figs. 7, 8). Net calcification reflects gross calcification and gross dissolution, so it is not abnormal to see net calcification decoupled from physiological or geochemical data. However, from our data it seems that pH<sub>CF</sub> is not the limiting parameter of calcification.

If the Mg/Ca ratio reflects the  $[Ca]_{CF}$ , then the higher Mg/Ca ratio observed in the geniculate complexes suggests a lower  $[Ca]_{CF}$ . Then this lower calcium concentration appears to be compensated by an increase in the pH<sub>CF</sub> of the calcification fluid (Fig. 8). In contrast, the non-geniculate forms show lower Mg/Ca ratios, implying a higher  $[Ca]_{CF}$  and, correspondingly, a lower pH<sub>CF</sub>. This could imply a coupling between  $[Ca]_{CF}$  and pH<sub>CF</sub>, potentially through proton exchangers like  $Ca^{2+}$ -ATPase or other Ca concentrating mechanisms.

Building on previous studies on  $\delta^{13}C_{tissue}$ , we interpret the changes in  $\delta^{13}C_{mineral}$  to reflect changes in the source of DIC (Bergstrom et al., 2020). We suggest that higher photosynthetic activity (i.e. gross photosynthesis) observed for the geniculate species implies higher need for DIC to support both photosynthesis and calcification. To compensate for the higher  $CO_2$  drawdown of photosynthesis and support calcification other sources of DIC like  $CO_2$  diffusion or a better recycling of metabolic  $CO_2$  may be involved. Those sources would explain the lower  $\delta^{13}C_{mineral}$  in geniculate complexes compared to nongeniculate. Higher photosynthetic activity in the geniculate complexes would supply energy to the metabolism, the trade off potentially being DIC limited calcification.

On the other hand, non-geniculate complexes are relying on fast calcification, the lower photosynthesis activity might limit  $CO_2$  drawdown which will allow higher internal DIC availability and sustain higher calcification. The other argument for DIC being the limiting parameter is the non-variation of  $pH_{CF}$  with changing irradiance. While higher  $pH_{CF}$  can be achieved for the geniculate through higher photosynthesis activity, the  $pH_{CF}$  of non-geniculate complexes are also elevated relative to seawater despite lower photosynthesis activity.

Future research will benefit from indirect (e.g., proxies) and direct constraint (e.g., microelectrode) on DIC<sub>CF</sub> to test those hypotheses. The geochemical differences between morphologies we observed during this study reflect different photosynthetic strategies and metabolic needs of the organisms. Here we tried to draw some mechanistic explanation to the observed changes in calcification based on the geochemical differences between non-geniculate and geniculate complexes. We show that DIC<sub>CF</sub> is a limiting parameter to calcification, we hypothesized that geniculate species have greater passive CO<sub>2</sub> diffusion/recycling, while DIC is not as limiting for the non-geniculate due to better carbon concentration mechanisms and lower photosynthetic CO<sub>2</sub> drawdown which supports higher rates of calcification. The coralline red algae do present a certain plasticity in their carbon sources for DIC (Bergstrom et al., 2020) and regulation of pH<sub>CF</sub>, which can provide some resilience to changing environmental conditions. Additional studies on how coralline algae modulate DIC<sub>CF</sub> and pH<sub>CF</sub> would be helpful to capture the limits of plasticity of photosynthesis and calcification modulation under stressors such as ocean acidification or warming temperature. This understanding will be critical for assessing the impact of global changes on those foundational species.

#### 4.7 Does light impact proxies for paleoreconstruction?

Carbonate structures produced by coralline algae (e.g., rhodoliths, crusts) can be used as archives for paleoreconstruction (MacDonald et al., 2024). The main geochemical differences in our study are observed between the

different morphologies of coralline red algae. Nevertheless, non-geniculate (i.e., encrusting) species are much more commonly used for paleoenvironmental reconstructions, we will then focus on the non-geniculate complexes for the rest of this section.

As we observed,  $\delta^{11}$ B-derived pH<sub>CF</sub> is not impacted by light at the complex levels which does not produce additional complexity for the use of the proxy. Anagnostou et al. (2019) presented a robust calibration of the  $\delta^{11}$ B proxy based on culture experiments on a high-latitude crustose coralline red algae *Clathromorphum compactum*. As the carbonate archives usually are produced by a mix of species, a complex-specific response to ocean acidification and the strong control they exert on their calcification fluid could be a limitation of the proxy, but our findings suggest  $\delta^{11}$ B should be at least insensitive to light levels. This is especially true because encrusting species being anchored to the substrate should be less impacted by differential light exposure. Nevertheless, with the increasing availability in species-specific geochemical data, a rigorous approach may involve using DNA-based identification within the core to calibrate geochemical records.

Despite significant relationships for Mg/Ca (*Pneophyllum complex* and *Phymatolithopsis complex*) and Li/Ca (*Pneophyllum complex*), Li/Mg ratios did not show any significant effect of changing irradiance, which does not impair the applicability of the temperature proxy for both species. Also, no significant differences were observed for the Li/Ca of the two non-geniculate species. Our results on mid-latitude low-light adapted species show that light does not impair the application of the  $\delta^{11}B$  and Li/Mg proxies.

Coralline red algae species are adapted to environments where light availability can vary (e.g. latitude, depth). While the results of this study may be applicable to mid-latitude species, it might not be transferable to coralline algae from other latitudes, for example, it has been shown that Arctic species rely on stored photosynthates to support winter calcification (Adey et al., 2019; Gould et al., 2022) which could influence the geochemical parameters.

#### 5 Conclusions

The geochemistry ( $\delta^{11}$ B,  $\delta^{13}$ C<sub>mineral</sub> and trace elements) of four low-light adapted complexes of coralline red algae cultured under different irradiances was investigated in this study following prior work by Krieger et al. (2023). Two morphologies were investigated: geniculate (branching) complexes, *Corallina/Arthrocardia robust* and *Corallina/Arthrocardia fine* and non-geniculate (encrusting/mounding) complexes, *Pneophyllum complex* and *Phymatolithopsis complex*.

The first purpose of this study was to investigate the effect of light (changing irradiance) on the pH of calcification for the different complexes. Based on photophysiological parameters (i.e. gross photosynthesis, ETR max) and  $\delta^{13}C_{mineral}$ , we show that at the complex levels photosynthesis activity has an impact on the geochemical signature of the mineral. However, despite increasing photosynthetic activity with irradiance,  $\delta^{11}B$  or pH<sub>CF</sub> was maintained constant for all treatments. pH<sub>CF</sub> was upregulated relative to seawater in all complexes with complex-specific pH<sub>CF</sub>. No significant effect of light was observed at the complex level in the range of irradiance (0.6-2.3) photons m<sup>-2</sup> d<sup>-1</sup>.

The main differences in physiological and geochemical parameters are observed between morphologies. Those results demonstrate two calcification regimes. We show that non-geniculate complexes have higher net calcification, higher  $\delta^{13}C_{mineral}$ , lower gross photosynthesis, lower pH<sub>CF</sub>, lower Mg/Ca while geniculate have lower net calcification, lower  $\delta^{13}C_{mineral}$ , higher gross photosynthesis, higher pH<sub>CF</sub>, higher Mg/Ca.

We highlight that  $pH_{CF}$  can be positively influenced via photosynthetic regimes inherent to morphologies. We show that net calcification is decoupled from  $pH_{CF}$  and that based on Mg/Ca, changes in  $pH_{CF}$  are compensated by changes in  $[Ca]_{CF}$ . The main differences between calcification modes is likely due to DIC and carbon concentrating mechanisms reflected in our data by  $\delta^{13}C_{mineral}$ . The lower  $\delta^{13}C_{mineral}$  of geniculate species can indicate a relatively more important contribution of passive  $CO_2$  diffusion and/or higher recycling of  $CO_2$  to the DIC pool.

Higher calcification in non-geniculate complexes is supported by higher DIC<sub>CF</sub> due to lower CO<sub>2</sub> drawdown from photosynthesis and efficient carbon-concentrating mechanisms. Additionally, despite lower photosynthetic activity compared to geniculate complexes, photosynthesis-independent processes may help maintain elevated pH<sub>CF</sub> reducing the energetic cost of pH regulation. In contrast, geniculate complexes experience greater CO<sub>2</sub> drawdown limiting DIC<sub>CF</sub> use for calcification. Although CO<sub>2</sub> recycling or passive diffusion may partly offset this limitation, the energy obtained from photosynthesis in geniculate complexes is likely prioritized to other metabolic needs at the expense of calcification. These differences could be explained by the competition experienced by non-geniculate species to not be overgrown (e.g. turf algae) which must also rely on fast calcification while geniculate species must compensate for a more dynamic environment and prioritize other needs (e.g. grazing, repairs) (Stenneck et al., 1986; Connell, 2003b; Edwards and Connell, 2012).

No effect of irradiance is observed on the temperature proxy Li/Mg for the different complexes in the range of irradiances tested in this study. Light should not add additional complexity to the interpretation of the Li/Mg and  $\delta^{11}B$  proxies when applied to paleoreconstruction studies from rhodolith beds.

Development of proxies to derive a second carbonate parameter in high Mg calcite such as the  $[CO_3^{2-}]_{CF}$  proxies (e.g. B/Ca, U/Ca) developed in the aragonitic corals as well as direct microelectrode measurements of the calcifying parameters (e.g. pH<sub>CF</sub>, DIC<sub>CF</sub>) will be relevant to study the dynamics of the calcification space in coralline red algae.

This study demonstrates variability in responses of coralline red algae under irradiance and highlights distinct biomineralization mechanisms between branching (geniculate) and encrusting (non-geniculate) mid-latitude low-light adapted complexes. Photosynthesis impacts the availability and source of DIC<sub>CF</sub> which has implications on calcification. In the perspective of calcification, plasticity on DIC sources is determinant for acclimation of coralline red algae. Further research should be done on coralline algal species that experience different irradiance regimes and environments (e.g. latitude, depth). Additional study on the joint effect of ocean acidification and changing irradiance might provide some interesting dynamics and will be needed to understand the full implications of future global changes and associated perturbations on the coralline algae communities and dependent ecosystems.

- Acknowledgement: We want to thank the reviewers for their constructive comments on this manuscript. We thank Seth John,
- Josh West, Shun-Chun Yang for technical support and use of the Neptune at the Dornsife Plasma facility at University of
- 506 Southern California. We thank Céline Liorzou, Marie-Laure Rouget, Bleuenn Guéguen, Oanez Lebeau, Fabien Dewilde for
- 507 technical support and use of the instruments at the Pôle Spectrométrie Océan at the Institut Européen de la Mer (Plouzané,
- 508 France).

509

- Funding sources: This work was funded by a grant from the David and Lucile Packard Foundation (grant no. 85180), National
- 511 Science Foundation grant no. NSF-RISE-2024426, and by gifts from Ocean kind and Dalio Philanthropies. The Center for
- 512 Diverse Leadership in Science is also supported by grant no. NSF-RISE-2228198, the Waverley Street Foundation, and the
- 513 Sloan Foundation.

514

- Author contributions: C.C. and R.A.E. conceived the project. C.C and R.A.E directed the research. E. K. and C.C. performed
- 516 culturing experiments, specimen characterization. M.G. performed isotope and trace element analyses at USC and IUEM. M.G.
- and J.G. performed statistical analyses and figures. M.G., R.A.E., C.C., and E.K. interpreted the geochemical data. M.G. wrote
- 518 the manuscript with input from R.A.E., C.C and E.K. All authors read and edited the manuscript.

519

- 520 Conflicts of Interest: The authors declare no conflict of interest. The funders had no role in the design of the study; in the
- 521 collection, analyses, or interpretation of data; in the writing of the manuscript, or in the decision to publish the results.

#### 522 References

- 523 Adey, H., W., Halfar, J., & Williams, B.: The Coralline Genus Clathromorphum Foslie emend. Adey, Biological,
- 524 Physiological, and Ecological Factors Controlling Carbonate Production in an Arctic-Subarctic Climate Archive,
- 525 Smithsonian Institution Scholarly Press, 2019.
- 526 Al-Horani, F. A., Al-Moghrabi, S. M., and De Beer, D.: The mechanism of calcification and its relation to photosynthesis and
- 527 respiration in the scleractinian coral Galaxea fascicularis, Mar Biol, 142, 419–426, https://doi.org/10.1007/s00227-002-0981-
- 528 8, 2003.
- 529 Anagnostou, E., Williams, B., Westfield, I., Foster, G. L., and Ries, J. B.: Calibration of the pH-δ<sup>11</sup>B and temperature-Mg/Li
- proxies in the long-lived high-latitude crustose coralline red alga Clathromorphum compactum via controlled laboratory
- 531 experiments, Geochim Cosmochim Acta, 254, 142–155, https://doi.org/10.1016/j.gca.2019.03.015, 2019.
- Anthony, K. R. N., Kline, D. I., Diaz-Pulido, G., Dove, S., Hoegh-Guldberg, O., Designed, -G, and Performed, -P: Ocean
- 533 acidification causes bleaching and productivity loss in coral reef builders, PNAS, 105, 17442–17446, 2008.

- Bergstrom, E., Ordoñez, A., Ho, M., Hurd, C., Fry, B., and Diaz-Pulido, G.: Inorganic carbon uptake strategies in coralline
- 535 algae: Plasticity across evolutionary lineages under ocean acidification and warming, Mar Environ Res, 161,
- 536 https://doi.org/10.1016/j.marenvres.2020.105107, 2020.
- 537 Bessell-Browne, P., Negri, A. P., Fisher, R., Clode, P. L., and Jones, R.: Impacts of light limitation on corals and crustose
- 538 coralline algae, Sci Rep, 7, https://doi.org/10.1038/s41598-017-11783-z, 2017.
- 539 Borowitzka, M. A., & Larkum, A. W. D.: Calcification in algae: Mechanisms and the role of metabolism, Critical Reviews in
- 540 Plant Sciences, 6(1), 1–45, https://doi.org/10.1080/07352688709382246, 1987.
- 541 Cameron, L. P., Reymond, C. E., Bijma, J., Büscher, J. V., De Beer, D., Guillermic, M., Eagle, R. A., Gunnell, J., Müller-
- Lundin, F., Schmidt-Grieb, G. M., Westfield, I., Westphal, H., and Ries, J. B.: Impacts of Warming and Acidification on Coral
- 543 Calcification Linked to Photosymbiont Loss and Deregulation of Calcifying Fluid pH, J Mar Sci Eng, 10,
- 544 https://doi.org/10.3390/jmse10081106, 2022.
- 545 Comeau, S., Carpenter, R. C., and Edmunds, P. J.: Effects of irradiance on the response of the coral Acropora pulchra and the
- 546 calcifying alga Hydrolithon reinboldii to temperature elevation and ocean acidification, J Exp Mar Biol Ecol, 453, 28–35,
- 547 https://doi.org/10.1016/j.jembe.2013.12.013, 2014.
- 548 Comeau, S., Cornwall, C. E., Pupier, C. A., DeCarlo, T. M., Alessi, C., Trehern, R., and McCulloch, M. T.: Flow-driven micro-
- 549 scale pH variability affects the physiology of corals and coralline algae under ocean acidification, Sci Rep, 9,
- 550 https://doi.org/10.1038/s41598-019-49044-w, 2019.
- 551 Connell, S. D.: The monopolization of understorey habitat by subtidal encrusting coralline algae: A test of the combined effects
- of canopy-mediated light and sedimentation, Mar Biol, 142, 1065–1071, https://doi.org/10.1007/s00227-003-1021-z, 2003b.
- 553 Cornwall, C. E., Hepburn, C. D., Pilditch, C. A., and Hurd, C. L.: Concentration boundary layers around complex assemblages
- of macroalgae: Implications for the effects of ocean acidification on understory coralline algae, Limnol Oceanogr, 58, 121–
- 555 130, https://doi.org/10.4319/lo.2013.58.1.0121, 2013.
- 556 Cornwall, C. E., Boyd, P. W., McGraw, C. M., Hepburn, C. D., Pilditch, C. A., Morris, J. N., Smith, A. M., and Hurd, C. L.:
- 557 Diffusion boundary layers ameliorate the negative effects of ocean acidification on the temperate coralline macroalga
- Arthrocardia corymbosa, PLoS One, 9, https://doi.org/10.1371/journal.pone.0097235, 2014.
- 559 Cornwall, C. E., Comeau, S., and McCulloch, M. T.: Coralline algae elevate pH at the site of calcification under ocean
- acidification, Glob Chang Biol, 23, 4245–4256, https://doi.org/10.1111/gcb.13673, 2017.

- 561 Cornwall, C. E., Comeau, S., DeCarlo, T. M., Moore, B., D'Alexis, Q., and McCulloch, M. T.: Resistance of corals and
- 562 coralline algae to ocean acidification: Physiological control of calcification under natural pH variability, Proceedings of the
- Royal Society B: Biological Sciences, 285, https://doi.org/10.1098/rspb.2018.1168, 2018.
- Cornwall, C. E., Diaz-Pulido, G., and Comeau, S.: Impacts of ocean warming on coralline algal calcification: Meta-analysis,
- knowledge gaps, and key recommendations for future research, https://doi.org/10.3389/fmars.2019.00186, 2019.
- 566 Cornwall, C. E., Carlot, J., Branson, O., Courtney, T. A., Harvey, B. P., Perry, C. T., Andersson, A. J., Diaz-Pulido, G.,
- Johnson, M. D., Kennedy, E., Krieger, E. C., Mallela, J., McCoy, S. J., Nugues, M. M., Quinter, E., Ross, C. L., Ryan, E.,
- 568 Saderne, V., and Comeau, S.: Crustose coralline algae can contribute more than corals to coral reef carbonate production,
- 569 Commun Earth Environ, 4, https://doi.org/10.1038/s43247-023-00766-w, 2023.
- 570 DeCarlo, T. M., Holcomb, M., & McCulloch, M. T.: Reviews and syntheses: Revisiting the boron systematics of aragonite
- and their application to coral calcification, *Biogeosciences*, 15(9), 2819–2834, https://doi.org/10.5194/bg-15-2819-2018,
- 572 2018b.
- 573 Dissard, D., Douville, E., Reynaud, S., Juillet-Leclerc, A., Montagna, P., Louvat, P., and McCulloch, M.: Light and
- 574 temperature effects on δ11B and B / Ca ratios of the zooxanthellate coral Acropora sp.: Results from culturing experiments,
- 575 Biogeosciences, 9, 4589–4605, https://doi.org/10.5194/bg-9-4589-2012, 2012.
- 576 D'Olivo, J. P. and McCulloch, M. T.: Response of coral calcification and calcifying fluid composition to thermally induced
- 577 bleaching stress, Sci Rep, 7, https://doi.org/10.1038/s41598-017-02306-x, 2017.
- 578 Donald, H. K., Ries, J. B., Stewart, J. A., Fowell, S. E., and Foster, G. L.: Boron isotope sensitivity to seawater pH change in
- 579 a species of Neogoniolithon coralline red alga, Geochim Cosmochim Acta, 217, 240-253,
- 580 https://doi.org/10.1016/j.gca.2017.08.021, 2017.
- Eagle, R. A., Guillermic, M., De Corte, I., Alvarez Caraveo, B., Bove, C. B., Misra, S., Cameron, L. P., Castillo, K. D., and
- 582 Ries, J. B.: Physicochemical Control of Caribbean Coral Calcification Linked to Host and Symbiont Responses to Varying
- 583 pCO2 and Temperature, J Mar Sci Eng, 10, https://doi.org/10.3390/jmse10081075, 2022.
- 584 Edwards, M.S., Connell, S.D.: Competition, a Major Factor Structuring Seaweed Communities. In: Wiencke, C., Bischof, K.
- 585 (eds) Seaweed Biology. Ecological Studies, vol 219. Springer, Berlin, Heidelberg. https://doi.org/10.1007/978-3-642-28451-
- 586 **9 7**, 2012.

- 587 Egilsdottir, H., Olafsson, J., and Martin, S.: Photosynthesis and calcification in the articulated coralline alga Ellisolandia
- 588 elongata (Corallinales, Rhodophyta) from intertidal rock pools, Eur J Phycol, 51, 59-70,
- 589 https://doi.org/10.1080/09670262.2015.1101165, 2016.
- 590 Gabitov, R. I., Sadekov, A., & Leinweber, A.: Crystal growth rate effect on Mg/Ca and Sr/Ca partitioning between calcite and
- fluid: An in situ approach, Chemical Geology, 367, 70-82, 2014.
- 592 Gaillardet, J., Lemarchand, D., Göpel, C., and Manhès, G.: Evaporation and Sublimation of Boric Acid: Application for Boron
- 593 Purification from Organic Rich Solutions, The Journal of Geostandards and Geoanalysis, 2001.
- 594 Goreau, T. F.: Calcium carbonate deposition by coralline algae and corals in relation to their roles as reef-builders, Annals
- 595 New York Academy of Sciences, 109, 127–167, 1963.
- Gould, J., Halfar, J., Adey, W., & Ries, J. B.: Growth as a function of sea ice cover, light and temperature in the arctic/subarctic
- 597 coralline C. compactum: A year-long in situ experiment in the high arctic, Frontiers in Marine Science, 9, 2022,
- 598 https://doi.org/10.3389/fmars.2022.900033
- 599 GraphPad Prism version 10.2.3 for Windows, GraphPad Software, Boston, Massachusetts USA, www.graphpad.com
- 600 Guillermic, M., Misra, S., Eagle, R., Villa, A., Chang, F., and Tripati, A.: Seawater pH reconstruction using boron isotopes in
- multiple planktonic foraminifera species with different depth habitats and their potential to constrain pH and pCO<sub>2</sub> gradients,
- 602 Biogeosciences, 17, 3487–3510, https://doi.org/10.5194/bg-17-3487-2020, 2020.
- 603 Guillermic, M., Cameron, L. P., De Corte, I., Misra, S., Bijma, J., De Beer, D., Reymond, C. E., Westphal, H., Ries, J. B., and
- 604 Eagle, R. A.: Thermal stress reduces pocilloporid coral resilience to ocean acidification by impairing control over calcifying
- fluid chemistry, Sci. Adv, 2021.
- 606 Gutjahr, M., Bordier, L., Douville, E., Farmer, J., Foster, G. L., Hathorne, E. C., Hönisch, B., Lemarchand, D., Louvat, P.,
- 607 McCulloch, M., Noireaux, J., Pallavicini, N., Rae, J. W. B., Rodushkin, I., Roux, P., Stewart, J. A., Thil, F., and You, C. F.:
- 608 Sub-Permil Interlaboratory Consistency for Solution-Based Boron Isotope Analyses on Marine Carbonates, Geostand Geoanal
- Res, 45, 59–75, https://doi.org/10.1111/ggr.12364, 2021.
- 610 Halfar, J., Zack, T., Kronz, A., and Zachos, J. C.: Growth and high-resolution paleoenvironmental signals of rhodoliths
- 611 (coralline red algae): A new biogenic archive, J Geophys Res Oceans, 105, 22107–22116,
- 612 https://doi.org/10.1029/1999jc000128, 2000.

- 613 Hemming, N. G. and Hanson, G. N.: Boron isotopic composition and concentration in modern marine carbonates, Geochrmca
- 614 el Cosmochimica Ada, 537–543 pp., 1992.
- 615 Hofmann, L. C., Koch, M., and De Beer, D.: Biotic control of surface pH and evidence of light-induced H+ pumping and
- 616 Ca2+-H+ exchange in a tropical crustose coralline alga, PLoS One, 11, https://doi.org/10.1371/journal.pone.0159057, 2016.
- 617 Hofmann, L. C., Schoenrock, K., and de Beer, D.: Arctic coralline algae elevate surface pH and carbonate in the dark, Front
- 618 Plant Sci, 9, https://doi.org/10.3389/fpls.2018.01416, 2018.
- 619 Irving, A. D., Connell, S. D., and Elsdon, T. S.: Effects of kelp canopies on bleaching and photosynthetic activity of encrusting
- 620 coralline algae, J Exp Mar Biol Ecol, 310, 1–12, https://doi.org/10.1016/j.jembe.2004.03.020, 2004.
- 621 Juillet-Leclerc, A., Reynaud, S., Dissard, D., Tisserand, G., and Ferrier-Pagès, C.: Light is an active contributor to the vital
- effects of coral skeleton proxies, Geochim Cosmochim Acta, 140, 671–690, https://doi.org/10.1016/j.gca.2014.05.042, 2014.
- Kain, J. M.: Seasonal growth and photoinhibition in Plocamium cartilagineum (Rhodophyta) off the Isle of Man, Phycologia,
- 624 26(1), 88–99, <a href="https://doi.org/10.2216/i0031-8884-26-1-88.1">https://doi.org/10.2216/i0031-8884-26-1-88.1</a>, 1987.
- 625 Kamenos, N. A., Cusack, M., and Moore, P. G.: Coralline algae are global palaeothermometers with bi-weekly resolution,
- 626 Geochim Cosmochim Acta, 72, 771–779, https://doi.org/10.1016/j.gca.2007.11.019, 2008.
- 627 Klochko, K., Cody, G. D., Tossell, J. A., Dera, P., and Kaufman, A. J.: Re-evaluating boron speciation in biogenic calcite and
- 628 aragonite using <sup>11</sup>B MAS NMR, Geochim Cosmochim Acta, 73, 1890–1900, https://doi.org/10.1016/j.gca.2009.01.002, 2009.
- 629 Korbee, N., Navarro, N. P., García-Sánchez, M., Celis-Plá, P. S., Quintano, E., Copertino, M. S., Pedersen, A., Mariath, R.,
- 630 Mangaiyarkarasi, N., Pérez-Ruzafa, Figueroa, F. L., and Martínez, B.: A novel in situ system to evaluate the effect of high
- 631 CO2 on photosynthesis and biochemistry of seaweeds, Aquat Biol, 22, 245–259, https://doi.org/10.3354/ab00594, 2014.
- Krieger, E. C., Nelson, W. A., Grand, J., Le Ru, E. C., Bury, S. J., Cossais, A., Davy, S. K., and Cornwall, C. E.: The role of
- 633 irradiance in controlling coralline algal calcification, Limnol Oceanogr, 68, 1269–1284, https://doi.org/10.1002/lno.12345,
- 634 2023.
- 635 Liu, Y.-W., Sutton, J. N., Ries, J. B., and Eagle, R. A.: Regulation of calcification site pH is a polyphyletic but not always
- 636 governing response to ocean acidification, Sci Adv, 6, https://doi.org/10.1126/sciadv.aax1314, 2020.

- 637 MacDonald, E., Foster, G. L., Standish, C. D., Trend, J., Page, T. M., and Kamenos, N. A.: Historic ocean acidification of
- 638 Loch Sween revealed by correlative geochemical imaging and high-resolution boron isotope analysis of Boreolithothamniom
- 639 cf. soriferum, Earth Planet Sci Lett, 646, https://doi.org/10.1016/j.epsl.2024.118976, 2024.
- 640 Mao, J., Burdett, H. L., and Kamenos, N. A.: Efficient carbon recycling between calcification and photosynthesis in red
- coralline algae, Biol Lett, 20, https://doi.org/10.1098/rsbl.2023.0598, 2024.
- Martin, S., Cohu, S., Vignot, C., Zimmerman, G., and Gattuso, J. P.: One-year experiment on the physiological response of
- the Mediterranean crustose coralline alga, Lithophyllum cabiochae, to elevated pCO2 and temperature, Ecol Evol, 3, 676–693,
- 644 https://doi.org/10.1002/ece3.475, 2013a.
- 645 Martin, S., Charnoz, A., and Gattuso, J. P.: Photosynthesis, respiration and calcification in the Mediterranean crustose coralline
- 646 alga Lithophyllum cabiochae (Corallinales, Rhodophyta), Eur J Phycol, 48, 163–172,
- 647 https://doi.org/10.1080/09670262.2013.786790, 2013b.
- 648 McConnaughey, T. A., Bljrdeti-, J., Whelan, J. F., and Paull-, C. K.: Carbon isotopes in biological carbonates: Respiration
- and photosynthesis, Geochimica et Cosmochimica Acta, 1997.
- 650 McCoy, S. J., & Kamenos, N. A.: Coralline algae (Rhodophyta) in a changing world: Integrating ecological, physiological,
- and geochemical responses to global change, *Journal of Phycology*, 51(1), 6–24, 2015, https://doi.org/10.1111/jpy.12262
- 652 McCoy, S. J., Pueschel, C. M., Cornwall, C. E., Comeau, S., Kranz, S. A., Spindel, N. B., and Borowitzka, M. A.: Calcification
- 653 in the coralline red algae: a synthesis, https://doi.org/10.1080/00318884.2023.2285673, 2023.
- 654 McCulloch, M. T., D'Olivo, J. P., Falter, J., Holcomb, M., and Trotter, J. A.: Coral calcification in a changing World and the
- 655 interactive dynamics of pH and DIC upregulation, Nat Commun, 8, https://doi.org/10.1038/ncomms15686, 2017.
- 656 Michael, K., Ronnie, N. G., Jens, B., Rodney, R., and Søren, R.: Photosynthetic performance of surface-associated algae below
- 657 sea ice as measured with a pulse-amplitude-modulated (PAM) fluorometer and O2 microsensors, Mar Ecol Prog Ser, 223, 1–
- 658 14, 2001.
- Nguyen, H. T. T., Pritchard, D. W., Desmond, M. J., and Hepburn, C. D.: Coralline photosynthetic physiology across a steep
- light gradient, Photosynth Res, 153, 43–57, https://doi.org/10.1007/s11120-022-00899-7, 2022.
- 661 Noisette, F., Egilsdottir, H., Davoult, D., & Martin, S.: Physiological responses of three temperate coralline algae from
- 662 contrasting habitats to near-future ocean acidification, Journal of Experimental Marine Biology and Ecology, 448, 179–187,
- 663 2013, https://doi.org/10.1016/j.jembe.2013.07.006

- Pentecost, A.: Calcification and photosynthesis in corallina officinalis l. Using the 14co2 method, British Phycological Journal,
- 13, 383–390, https://doi.org/10.1080/00071617800650431, 1978.
- R Core Team (2021). R: A language and environment for statistical computing. R Foundation for Statistical Computing,
- Vienna, Austria. https://www.R-project.org/.
- 668 Roberts, R. D., Kühl, M., Glud, R. N., & Rysgaard, S.: Primary production of crustose coralline red algae in a high arctic
- 669 Fjord. Journal of Phycology, 38(2), 273-283, https://doi.org/10.1046/j.1529-8817.2002.01104.x, 2002.
- Sagert, S., Forster, R. M., Feuerpfeil, P., and Schubert, H.: Daily course of photosynthesis and photoinhibition in chondrus
- crispus (rhodophyta) from different shore levels, Eur J Phycol, 32, 363–371, https://doi.org/10.1080/09670269710001737299,
- 672 1997.
- 673 Steneck, R. S.: The Ecology of Coralline Algal Crusts: Convergent Patterns and Adaptative Strategies, Source: Annual Review
- of Ecology and Systematics, 273–303 pp., 1986.
- 675 Stewart, J. A., Christopher, S. J., Kucklick, J. R., Bordier, L., Chalk, T. B., Dapoigny, A., Douville, E., Foster, G. L., Gray,
- W. R., Greenop, R., Gutjahr, M., Hemsing, F., Henehan, M. J., Holdship, P., Hsieh, Y. Te, Kolevica, A., Lin, Y. P., Mawbey,
- 677 E. M., Rae, J. W. B., Robinson, L. F., Shuttleworth, R., You, C. F., Zhang, S., and Day, R. D.: NIST RM 8301 Boron Isotopes
- 678 in Marine Carbonate (Simulated Coral and Foraminifera Solutions): Inter-laboratory δ11B and Trace Element Ratio Value
- 679 Assignment, Geostand Geoanal Res, 45, 77–96, https://doi.org/10.1111/ggr.12363, 2021.
- 680 Sutton, J. N., Liu, Y. W., Ries, J. B., Guillermic, M., Ponzevera, E., and Eagle, R. A.: δ11B as monitor of calcification site pH
- in divergent marine calcifying organisms, Biogeosciences, 15, 1447–1467, https://doi.org/10.5194/bg-15-1447-2018, 2018.
- Wang, G., Cao, W., Yang, D., and Xu, D.: Variation in downwelling diffuse attenuation coefficient in the northern South
- 683 China Sea, Chinese Journal of Oceanology and Limnology, 26, 323–333, https://doi.org/10.1007/s00343-008-0323-x, 2008.
- Williams, B., Halfar, J., DeLong, K. L., Hetzinger, S., Steneck, R. S., & Jacob, D. E.: Multi-specimen and multi-site calibration
- of Aleutian coralline algal Mg/Ca to sea surface temperature, Geochimica et Cosmochimica Acta, 139, 190-204, 2014.
- Williams, S., Halfar, J., Zack, T., Hetzinger, S., Blicher, M., & Juul-Pedersen, T.: Comparison of climate signals obtained
- 687 from encrusting and free-living rhodolith coralline algae, Chemical Geology, 476, 418–428, 2018,
- 688 https://doi.org/10.1016/j.chemgeo.2017.11.038
- Zeebe, R. E. and Wolf-Gladrow, D.: CO<sub>2</sub> in Seawater: Equilibrium, Kinetics, Isotopes Elsevier Oceanography Series, No. 65,
- 690 Gulf Profe

**Figure Caption** Figure 1: Pictures of the four coralline red algae complexes used in this study (already presented in Krieger et al., 2023) and showing the different morphologies: non-geniculate (e.g. crustose) and geniculate (e.g. branching). Geniculate complexes: Corallina/Arthrocardia "robust" and Corallina/Arthrocardia "fine", non-geniculate complexes: Pneophyllum complex and Phymatolithopsis complex. Figure 2: Averages of photophysiological parameters of the four complexes from Krieger et al. (2023) against irradiances. A. Net calcification (mg<sub>CaCO3</sub>/cm<sup>2</sup>/day), B. Gross photosynthesis (µgO<sub>2</sub>/cm/h), C. Maximum electron transport rate, ETRmax, D. Photosynthetic efficiency measured by the "variable fluorescence" normalized to maximum fluorescence, Fv/Fm, E. Chlorophyll a, Chl a (mg/g). Averages are calculated from the full dataset from Krieger et al. (2023), error bars

**Figure 3:** Averages of geochemical data measured in this study against irradiances. A. Net calcification (mg<sub>CaCO3</sub>/cm<sup>2</sup>/day), B. boron isotopes of the mineral,  $\delta^{11}$ B (‰), C. carbon isotopes of the mineral  $\delta^{13}$ C<sub>mineral</sub> (‰), D. carbon isotopes of the

tissue  $\delta^{13}$ C<sub>tissue</sub> (‰) from Krieger et al. (2023), E. B/Ca of the mineral (umol/mol) and F. Mg/Ca of the mineral

are based on 2 SD. Regressions are shown in Fig. S2.

mmol/mol). Error bars are based on 2 SD. Regressions are shown in Fig. S1.

- Figure 4: Principal component analysis (PCA) of the geochemical and photo physiological data used in this study (a) loadings
- 733 and (b) biplot. Vectors present a positive relationship between ETRmax and irradiance, a negative relationship between net
- calcification and  $\delta^{11}$ B, positive relationships between net calcification and  $\delta^{13}$ C<sub>mineral</sub> and between  $\delta^{11}$ B and Fv/Fm.
- Geniculate and non-geniculate species cluster together. Non-geniculate complexes (*Pneophyllum complex* and
- *Phymatolithopsis complex*) show higher net calcification, higher  $\delta^{13}C_{mineral}$  and lower  $\delta^{11}B$ . Geniculate complexes
- 737 Corallina/Arthrocardia robust and Corallina/Arthrocardia fine on the contrary show lower net calcification, lower δ<sup>13</sup>C<sub>mineral</sub>
- 738 and higher  $\delta^{11}$ B.

739

- Figure 5: Multi-panel plots showing crossplots of  $\delta^{13}C_{mineral}$  (%) and  $\delta^{11}B$  (%). Averages are calculated based on this study
- for geochemical parameters and from the full dataset in Krieger et al. (2023). Individual paired data are also shown to
- maximize the information displayed, color scheme corresponds to the different irradiances. A. crossplot of  $\delta^{13}C_{mineral}$  (%)
- and  $\delta^{13}C_{tissue}$  (‰), linear significant relationships are shown with black lines, B.  $\delta^{11}B$  (‰) and  $\delta^{13}C_{mineral}$  (‰), C.  $\delta^{13}C_{mineral}$
- 744 (‰) and Net Calcification (mg<sub>CaCO3</sub>/cm²/day), D. δ<sup>11</sup>B (‰) and Net Calcification (mg<sub>CaCO3</sub>/cm²/day), E. δ<sup>13</sup>C<sub>mineral</sub> (‰)
- 745 and gross photosynthesis ( $\mu g O_2/cm/h$ ) and F.  $\delta^{11}B$  (‰) and gross photosynthesis ( $\mu g O_2/cm/h$ ).

746

- Figure 6: pH<sub>CF</sub> calculated from  $\delta^{11}$ B against irradiance for the four complexes, A. Corallina/Arthrocardia robust, B.
- 748 Corallina/Arthrocardia fine, C. Pneophyllum complex, D. Phymatolithopsis complex. Average values per treatment are
- presented with 2 SD error bars. Individual datapoints are also presented to assess variability within treatment.

750

- 751 **Figure 7:** Multi-panel plots showing crossplots of pH<sub>CF</sub>, A. net calcification (mg<sub>CaCO3</sub>/cm<sup>2</sup>/day), B. gross photosynthesis
- 752 (μgO<sub>2</sub>/cm/h), C. residual full-width-half-maximum, FWHM, D. δ<sup>13</sup>C<sub>mineral</sub> (‰) and E. Mg/Ca (mmol/mol). Large symbols
- show averages derived from full dataset from Krieger et al. (2023) while small colored symbols show individual paired data
- and irradiance level to display maximum information. Error bars are shown as 2 SD.

755

- Figure 8: Box plots comparing geniculate complexes (blue) and non-geniculate (green). Box plots show the median, 10, 90
- percentiles as well as the individual data points.

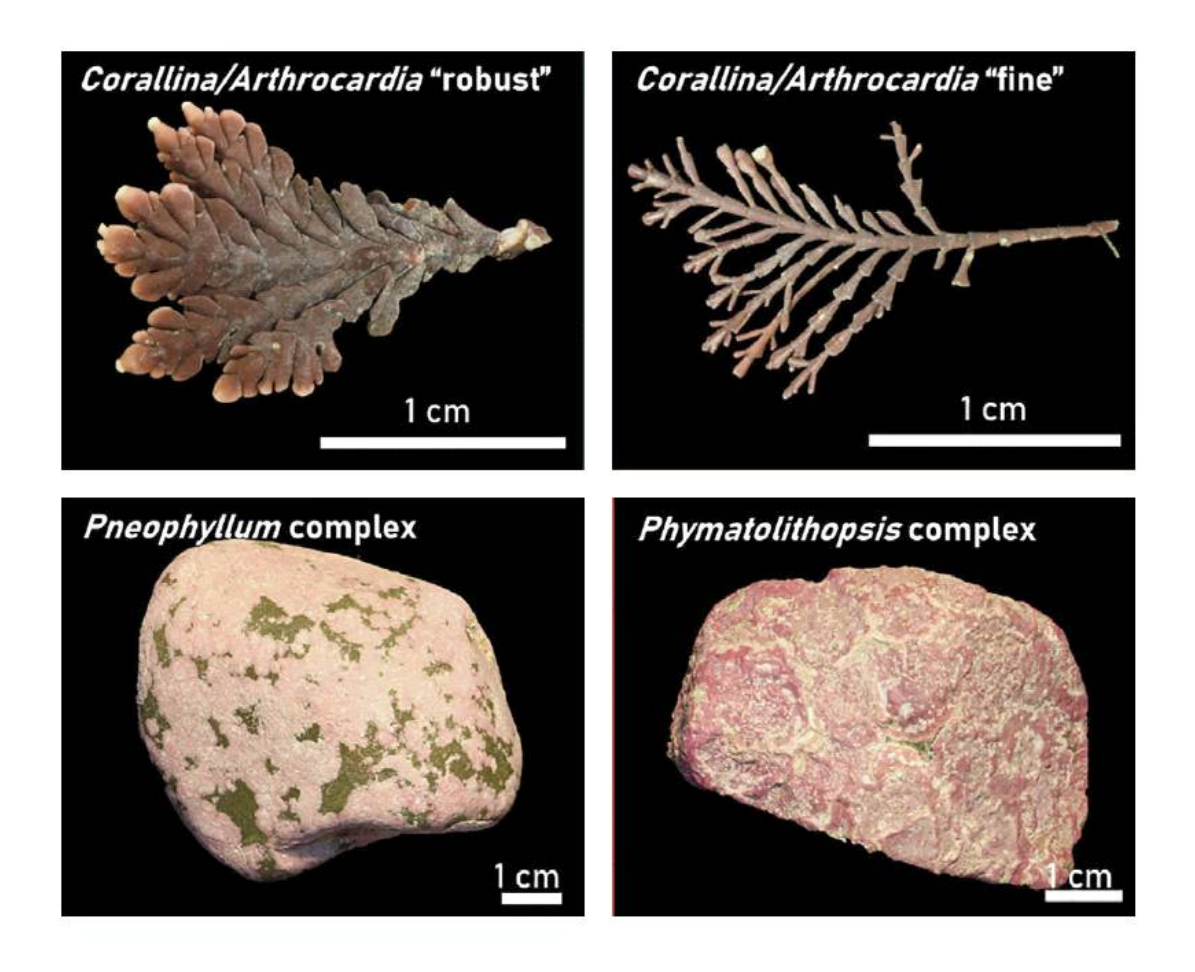


**Figure 1:** Pictures of the four coralline red algae complexes used in this study (already presented in Krieger et al., 2023) and showing the different morphologies: non-geniculate (e.g. crustose) and geniculate (e.g. branching). Geniculate complexes: *Corallina/Arthrocardia* "robust" and *Corallina/Arthrocardia* "fine", non-geniculate complexes: *Pneophyllum* complex and *Phymatolithopsis* complex.

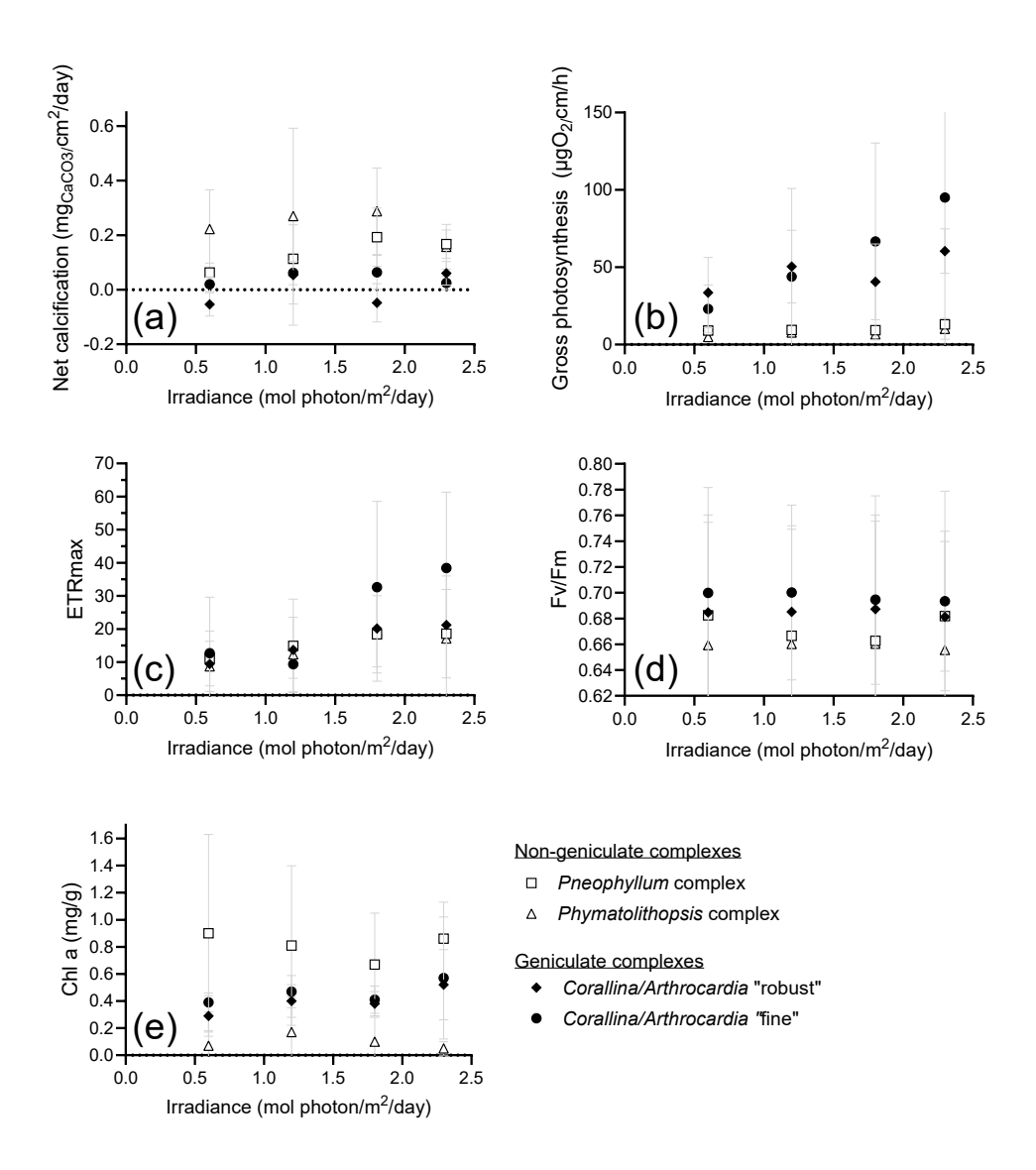


**Figure 2:** Averages of photophysiological parameters of the four complexes from Krieger et al. (2023) against irradiances. A. Net calcification (mg<sub>CaCO3</sub>/cm²/day), B. Gross photosynthesis (μgO₂/cm/h), C. Maximum electron transport rate, ETRmax, D. Photosynthetic efficiency measured by the "variable fluorescence" normalized to maximum fluorescence, Fv/Fm, E. Chlorophyll a, Chl a (mg/g). Averages are calculated from the full dataset from Krieger et al. (2023), error bars are based on 2 SD. Regressions are shown in Figure S2.

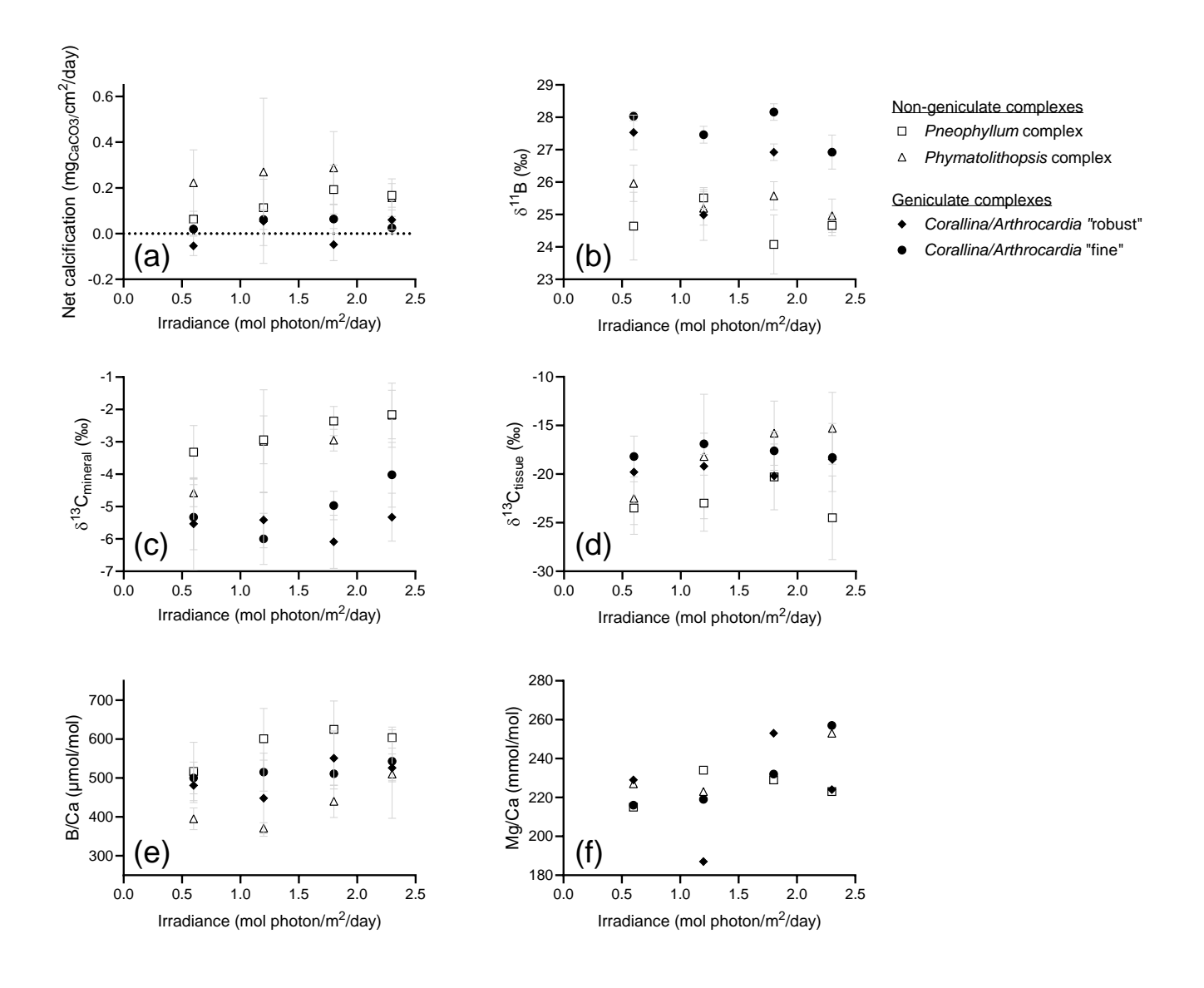
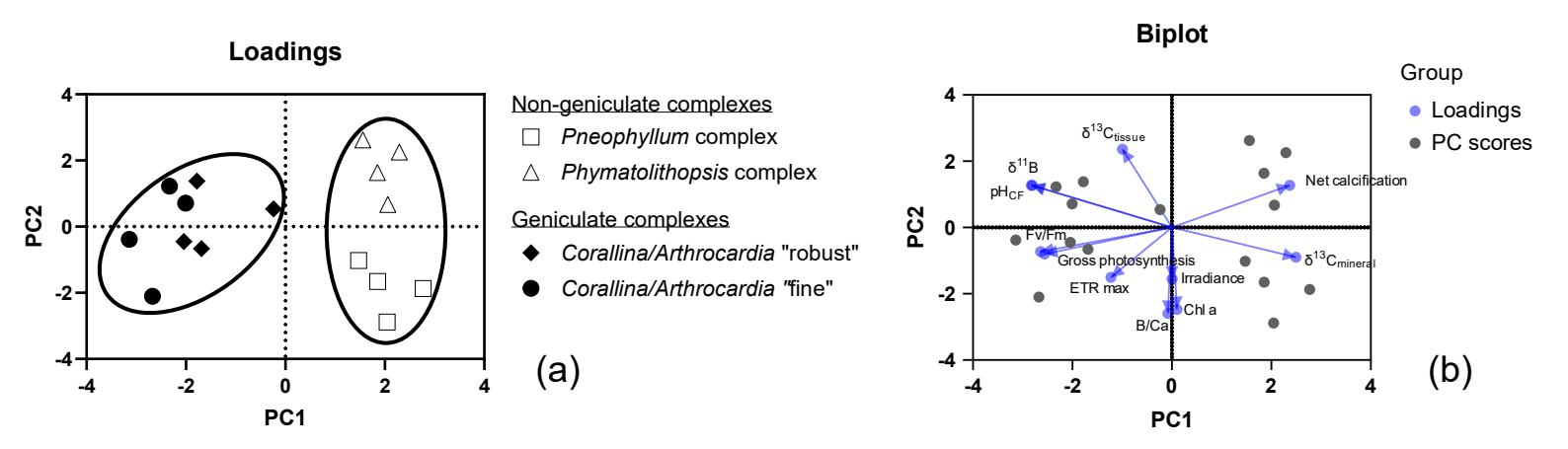
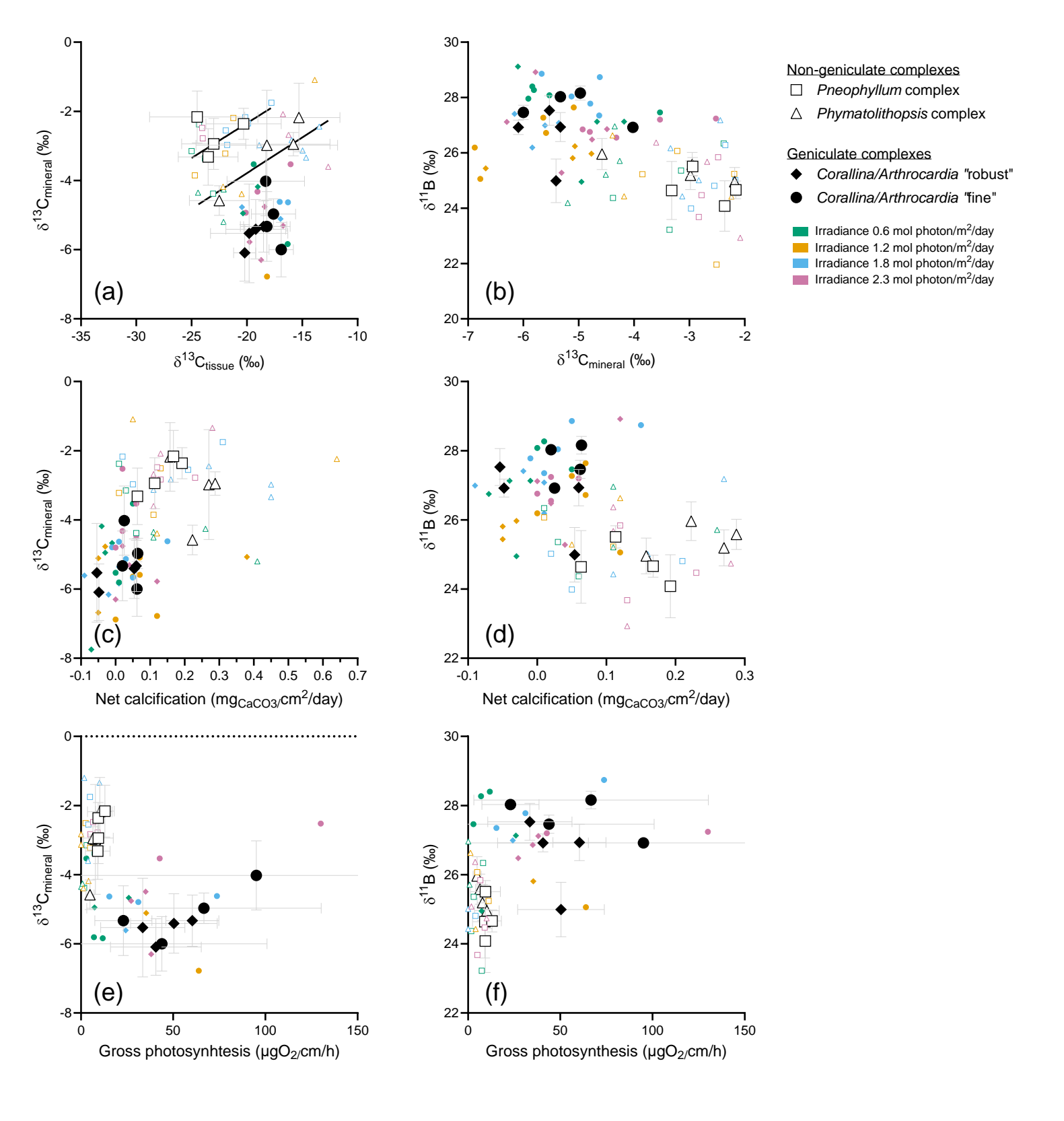


Figure 3: Averages of geochemical data measured in this study against irradiances. A. Net calcification ( $mg_{CaCO3}/cm^2/day$ ), B. boron isotopes of the mineral,  $\delta^{11}B$  (‰), C. carbon isotopes of the mineral  $\delta^{13}C_{mineral}$  (‰), D. carbon isotopes of the tissue  $\delta^{13}C_{tissue}$  (‰) from Krieger et al. (2023), E. B/Ca of the mineral ( $\mu$ mol/mol) and F. Mg/Ca of the mineral mmol/mol). Error bars are based on 2 SD. Regressions are shown in Figure S1.



**Figure 4:** Principal component analysis (PCA) of the geochemical and photo physiological data used in this study A. loadings and B. biplot. Vectors present a positive relationship between ETRmax and irradiance, a negative relationship between net calcification and  $\delta^{11}$ B, positive relationships between net calcification and  $\delta^{13}$ C<sub>mineral</sub> and between  $\delta^{11}$ B and Fv/Fm. Geniculate and non-geniculate species cluster together. Non-geniculate complexes (*Pneophyllum* complex and *Phymatolithopsis* complex) show higher net calcification, higher  $\delta^{13}$ C<sub>mineral</sub> and lower  $\delta^{11}$ B. Geniculate complexes *Corallina/Arthrocardia* robust and *Corallina/Arthrocardia* fine on the contrary show lower net calcification, lower  $\delta^{13}$ C<sub>mineral</sub> and higher  $\delta^{11}$ B.



**Figure 5:** Multi-panel plots showing crossplots of  $\delta^{13}C_{mineral}$  (‰) and  $\delta^{11}B$  (‰). Averages are calculated based on this study for geochemical parameters and from the full dataset in Krieger et al. (2023). Individual paired data are also shown to maximize the information displayed, color scheme corresponds to the different irradiances. A. crossplot of  $\delta^{13}C_{mineral}$  (‰) and  $\delta^{13}C_{tissue}$  (‰), linear significant relationships are shown with black lines, B.  $\delta^{11}B$  (‰) and  $\delta^{13}C_{mineral}$  (‰), C.  $\delta^{13}C_{mineral}$  (‰) and Net Calcification (mg<sub>CaCO3</sub>/cm²/day), D.  $\delta^{11}B$  (‰) and Net Calcification (mg<sub>CaCO3</sub>/cm²/day), E.  $\delta^{13}C_{mineral}$  (‰) and gross photosynthesis (μgO<sub>2</sub>/cm/h) and F.  $\delta^{11}B$  (‰) and gross photosynthesis (μgO<sub>2</sub>/cm/h).

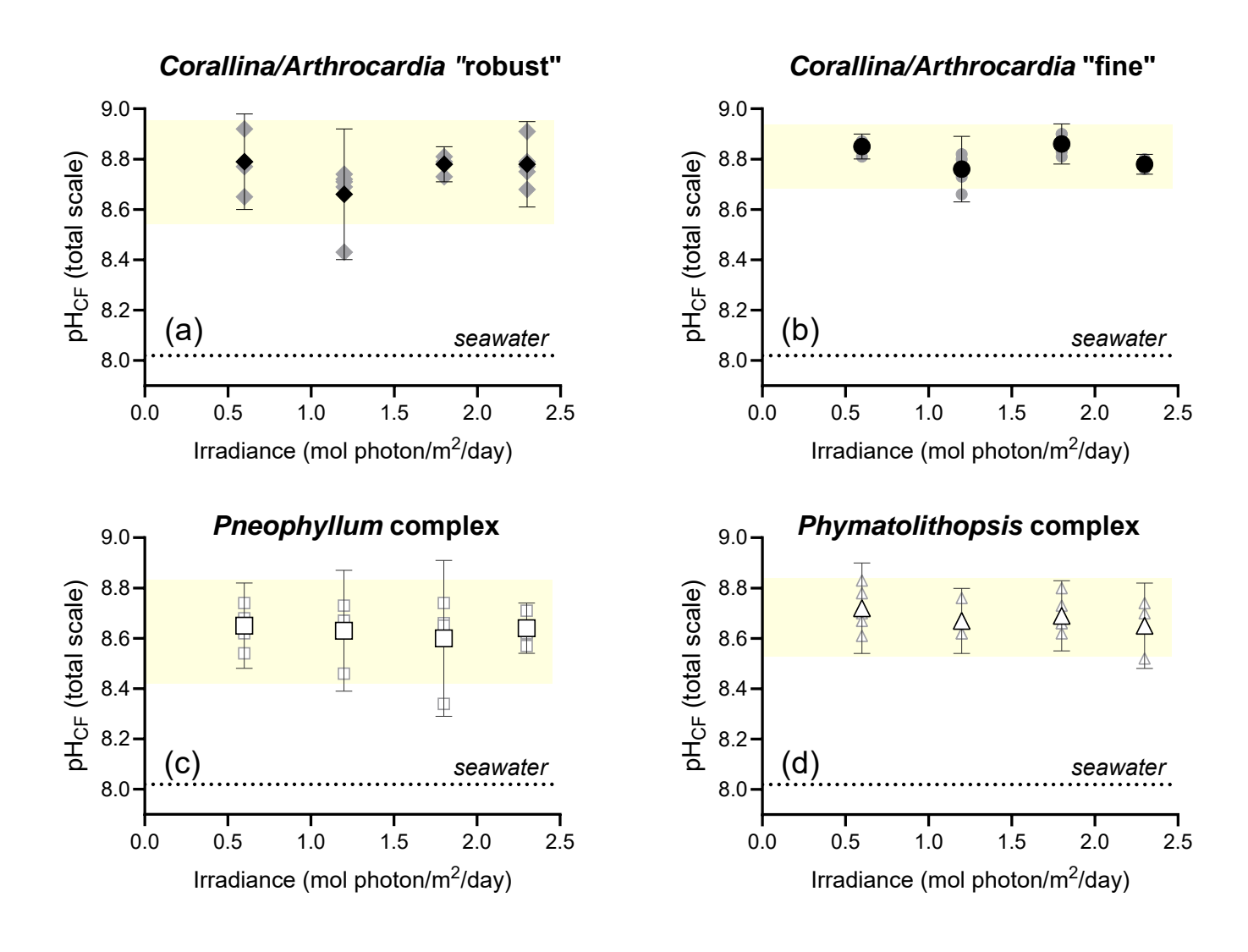


**Figure 6:** pH<sub>CF</sub> calculated from  $\delta^{11}$ B against irradiance for the four complexes, A. *Corallina/Arthrocardia* robust, B. *Corallina/Arthrocardia* fine, C. *Pneophyllum* complex, D. *Phymatolithopsis* complex. Average values per treatment are presented with 2 SD error bars. Individual datapoints are also presented to assess variability within treatment.

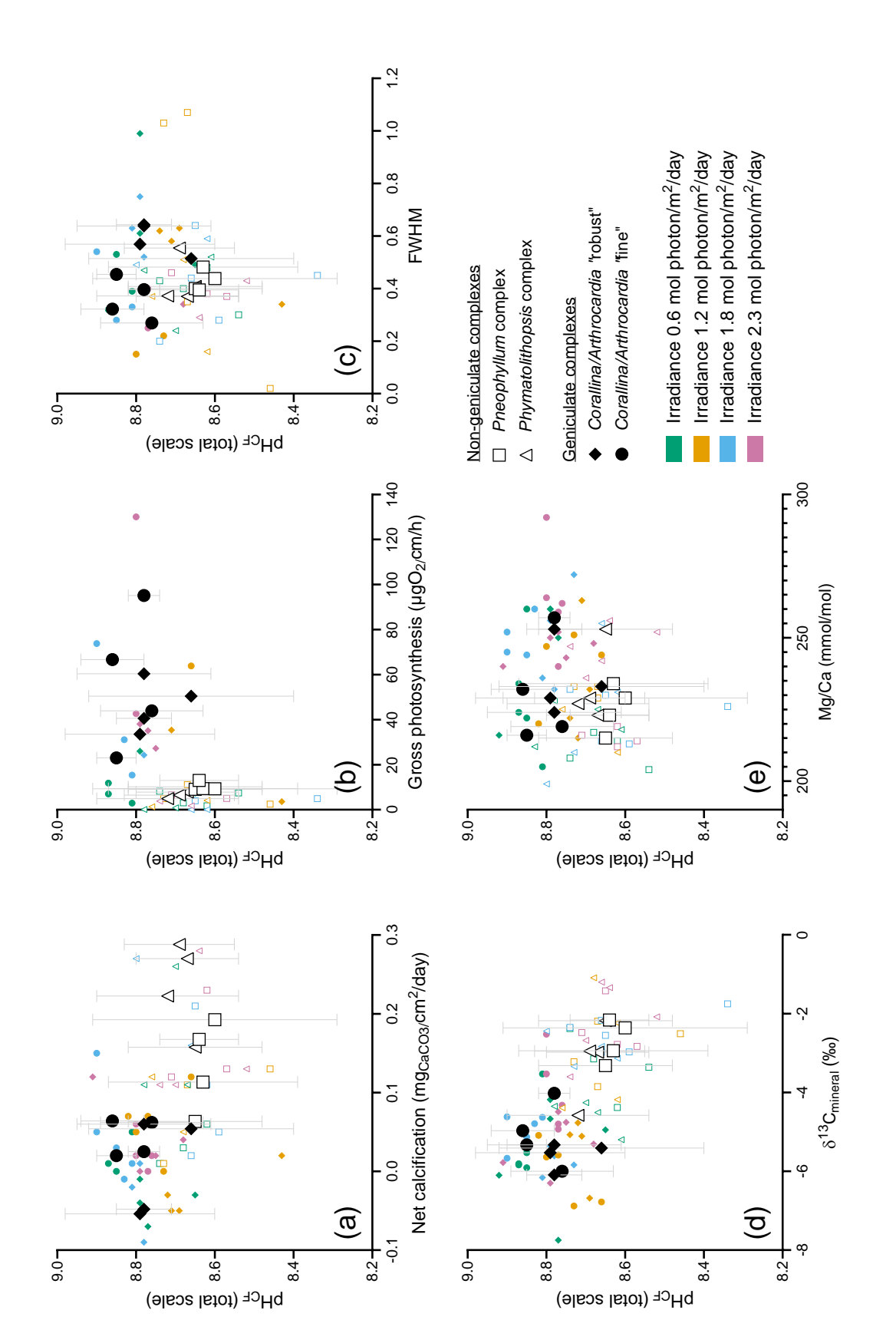
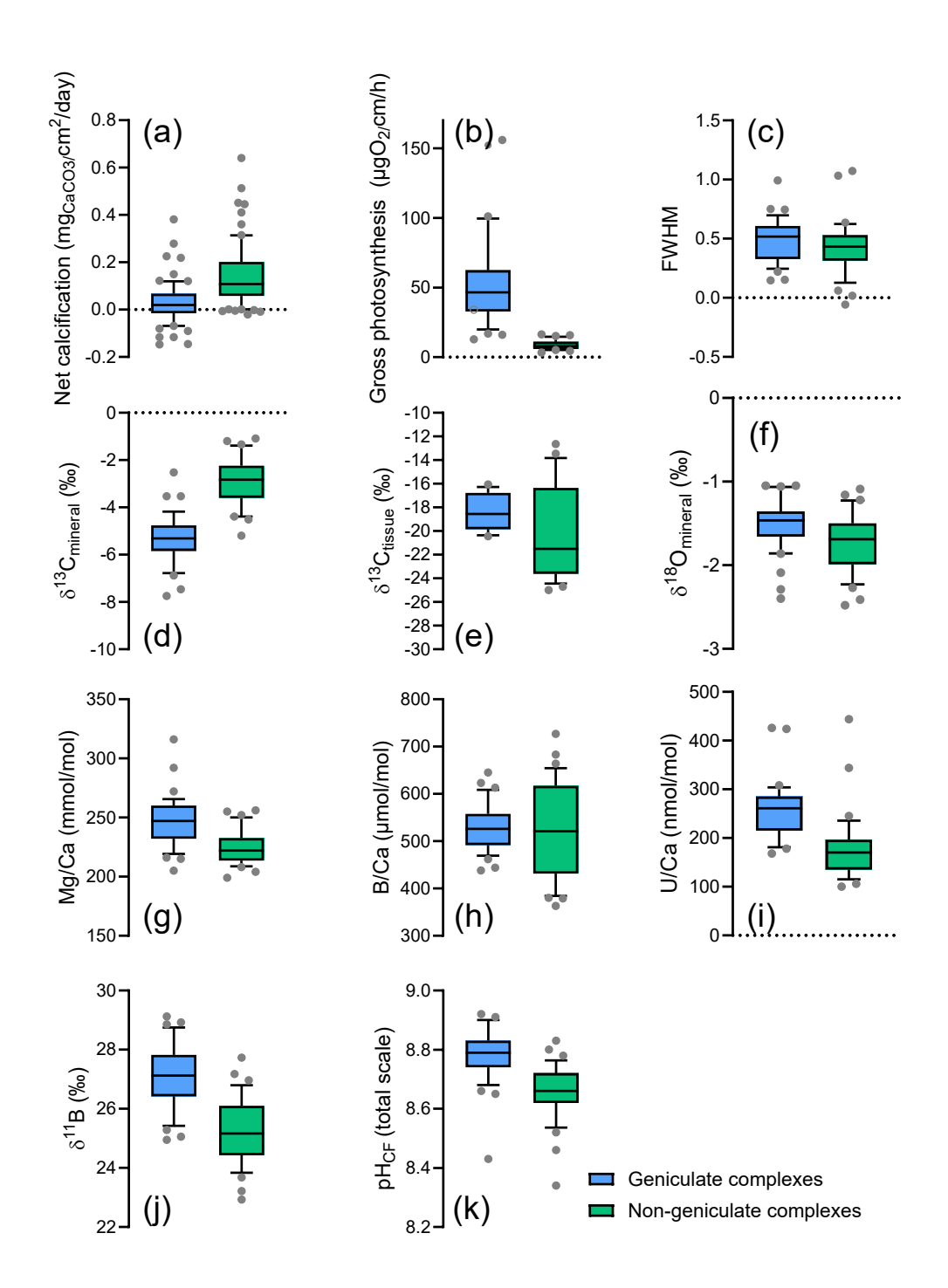


Figure 7: Multi-panel plots showing crossplots of pHcF, A. net calcification (mgCaCO3/cm2/day), B. gross photosynthesis (μgO2/cm/h), from full dataset from Krieger et al. (2023) while small colored symbols show individual paired data and irradiance level to display C. residual full-width-half-maximum, FWHM, D.  $\delta_{13}$ Cmineral (%) and E. Mg/Ca (mmol/mol). Large symbols show averages derived maximum information. Error bars are shown as 2 SD.



**Figure 8:** Box plots comparing geniculate complexes (blue) and non-geniculate (green). Box plots show the median, 10, 90 percentiles and as well as the individual data points.

# Supplement of

# The influence of irradiance and interspecific differences on $\delta^{11}B$ , $\delta^{13}C$ and elemental ratios in four coralline algae complexes

Maxence Guillermic et al.

Correspondence to: Maxence Guillermic (maxence.guillermic@gmail.com) and Robert Eagle (robeagle@g.ucla.edu)

#### **Supplemental Figures**

Figure S1: Data and significant models (black line) for the geochemical parameters measured and used in this study.

Figure S2: Data and significant models (black line) for the physiological parameters from Krieger et al. (2023) and used in this study.

**Figure S3:** Principal component analyses for (a) the relevant geochemical and physiological parameters used in this study and (b) elemental ratios and physiological parameters.

**Figure S4:** (a-d) Correlation matrices providing pairwise correlations between geochemical, and photo physiological data for a. *Corallina/Arthrocardia* "robust", b. Corallina/Arthrocardia "fine", c. *Pneophyllum* complex and d. *Phymatolithopsis* complex.

Figure S5: Correlation matrices for (a) the geniculate complexes and (b) the non-geniculate complexes.

**Figure S6:** Cross-plots of  $\delta^{13}$ C<sub>mineral</sub> and  $\delta^{11}$ B for other photo-physiological parameters, (a) and (b) Gross photosynthesis, (c) and (d) for ETRmax, (e) and (f) for Chl a.

**Figure S7:** Cross-plots of B/Ca with (a)  $\delta^{11}$ B and (b) Chl a.

#### **Supplemental Tables**

Table S1: Geochemical and physiological data.

Table S2: Comparison of linear and quadratic models based on AIC for the geochemical parameters measured in this study.

**Table S3:** Comparison of linear and quadratic models based on AIC for the physiological parameters published in Krieger et al., (2023).

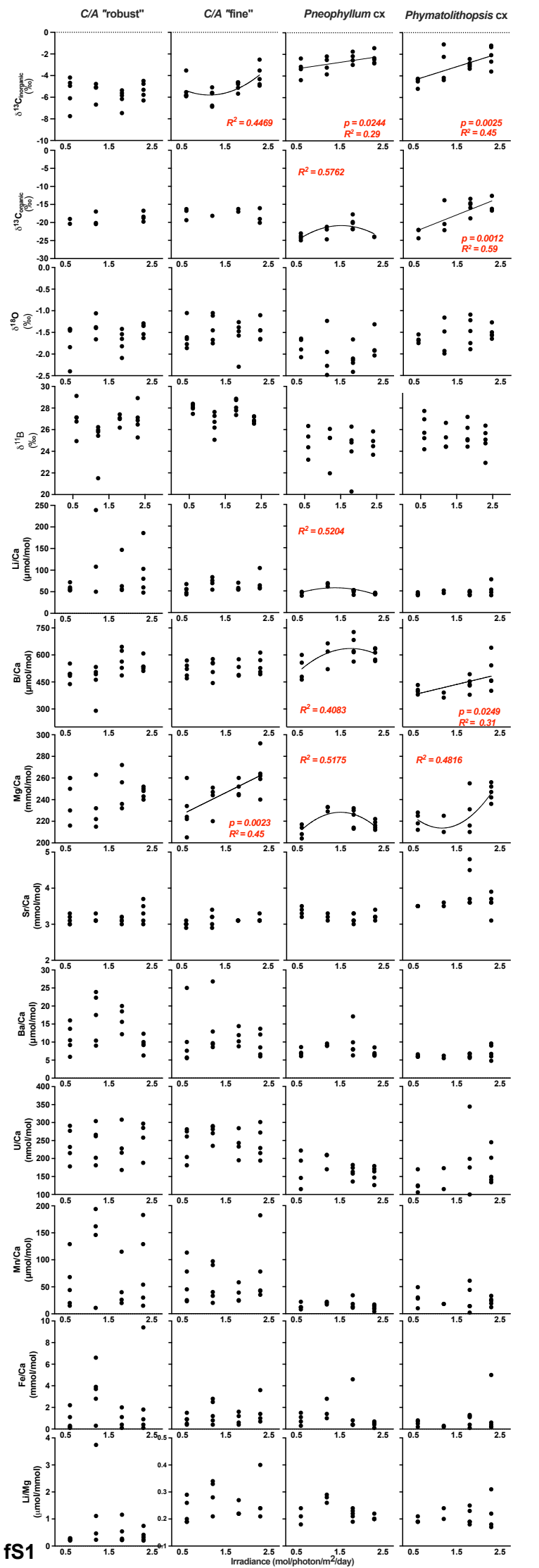
**Table S4:** ANOVA testing geochemical and physiological data against changing irradiance.

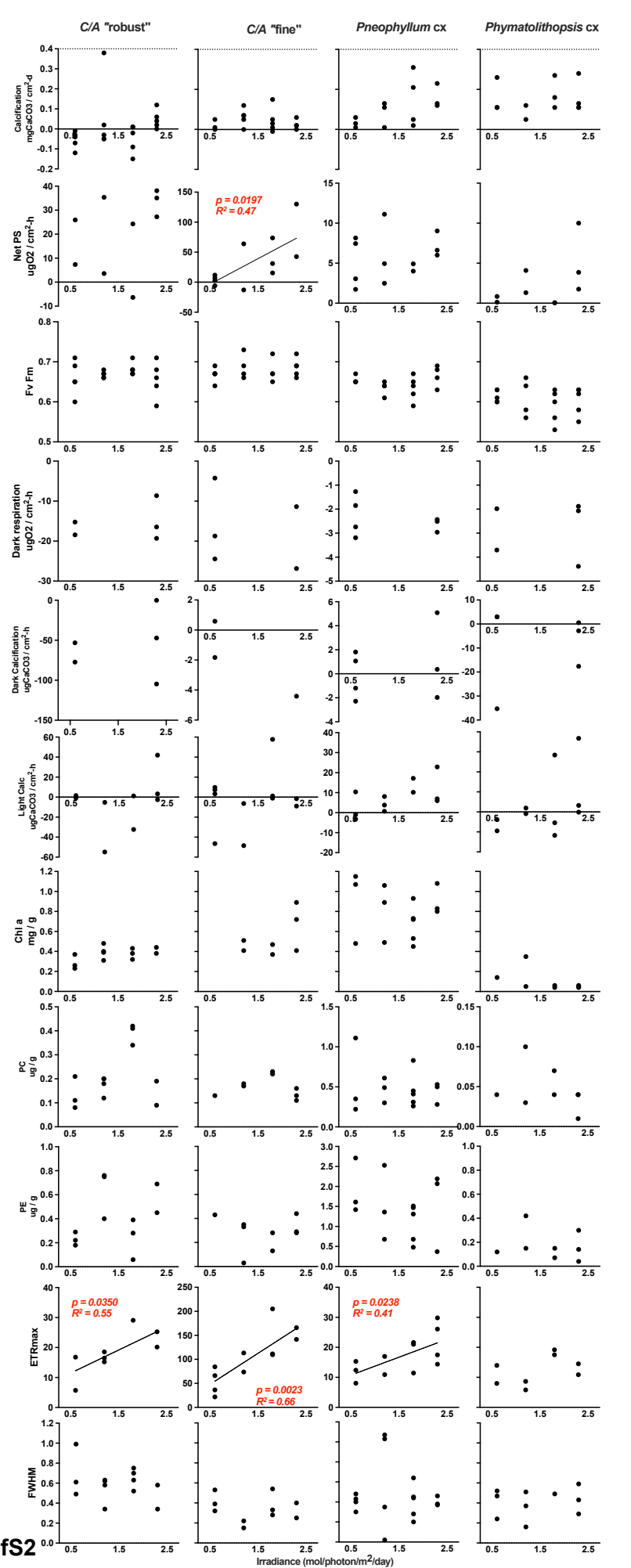
**Table S5:** T-test for parameters presenting significant ANOVA with changing irradiance (from Table S4).

**Table S6:** ANOVA testing geochemical and physiological data between complexes.

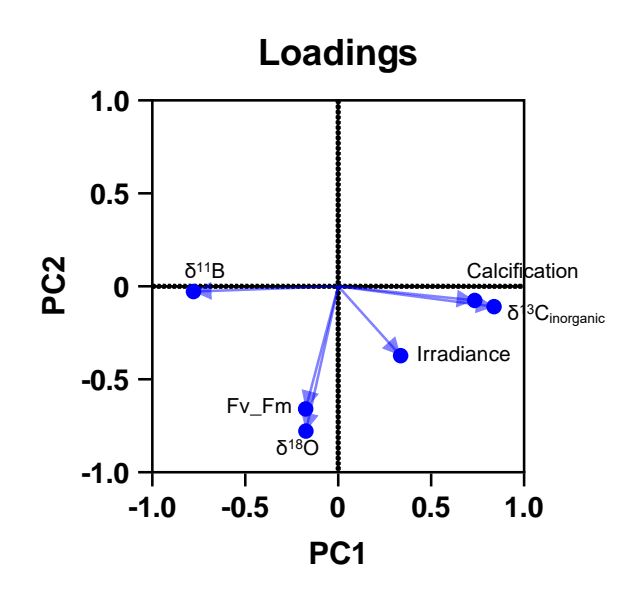
**Table S7:** T-test for parameters presenting significant ANOVA when testing for differences between complexes.

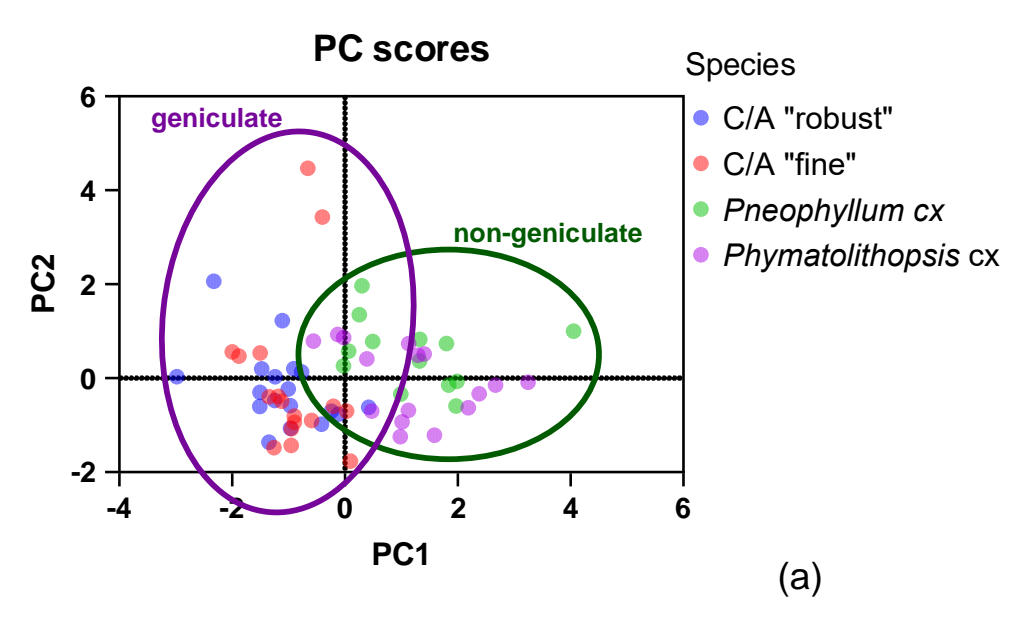
**Table S8:**  $\delta^{11}$ B of NIST 8301, JCp-1 and seawater measured in this study.



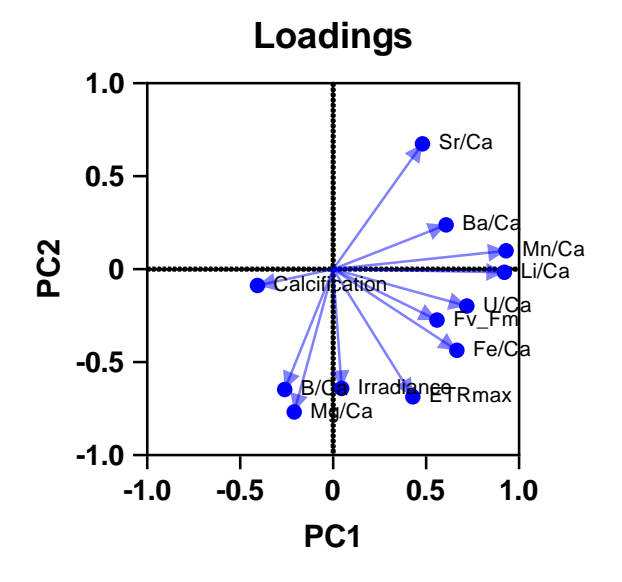


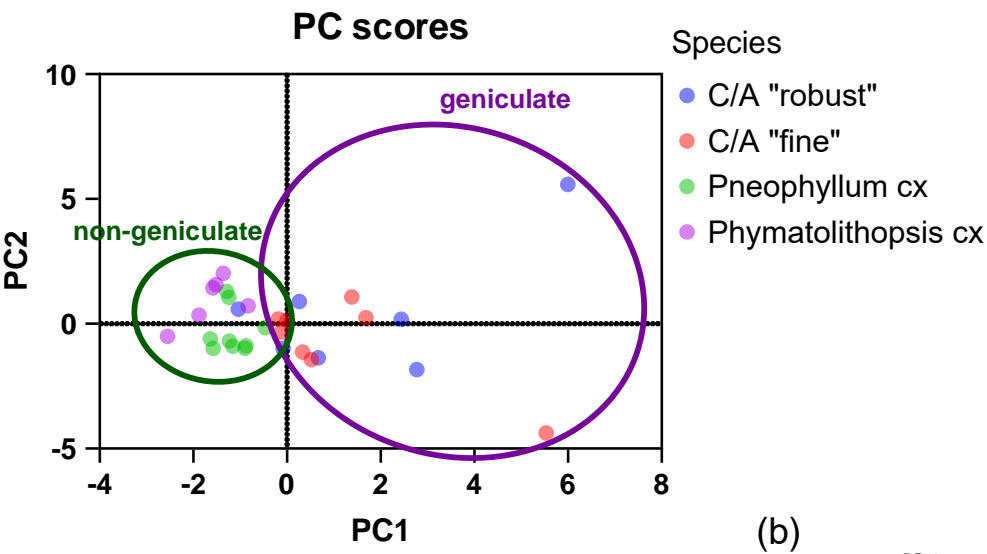
# **Physiological Data PCA**





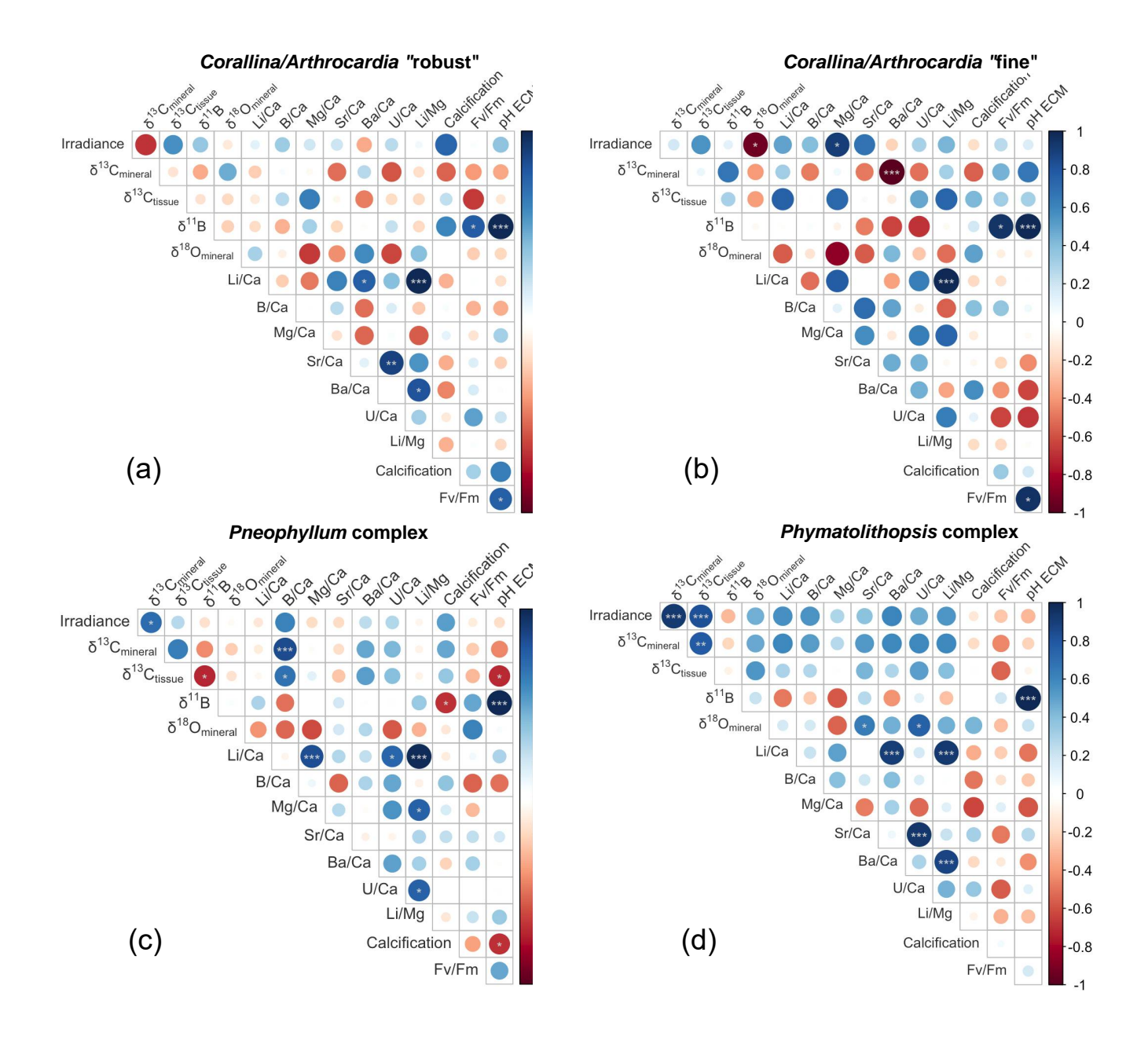
## **Trace Element Data PCA**





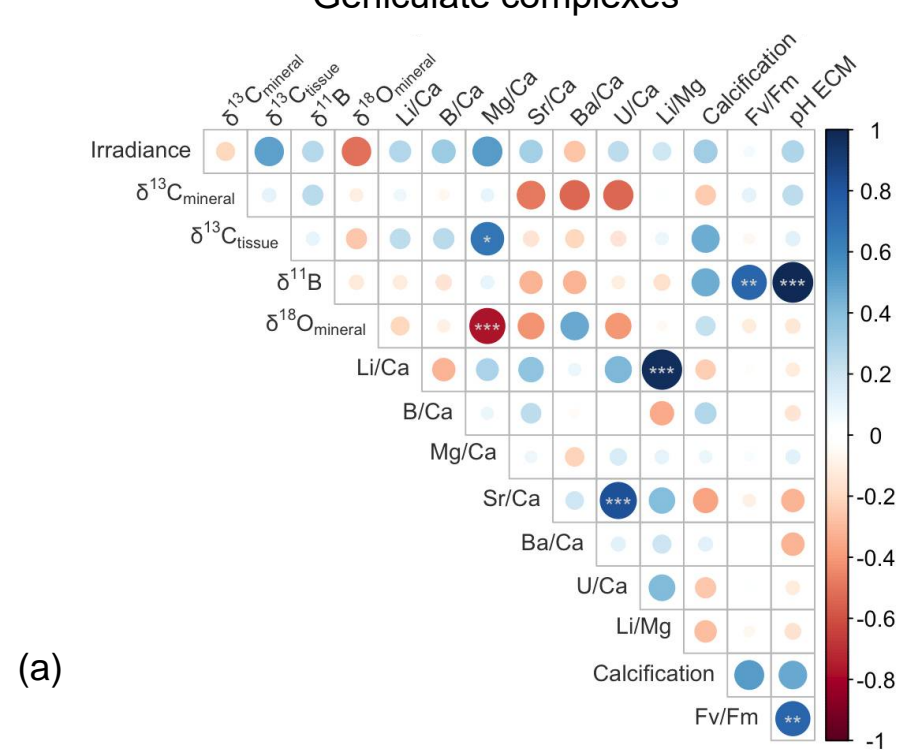
fS3

# **Correlation matrices**

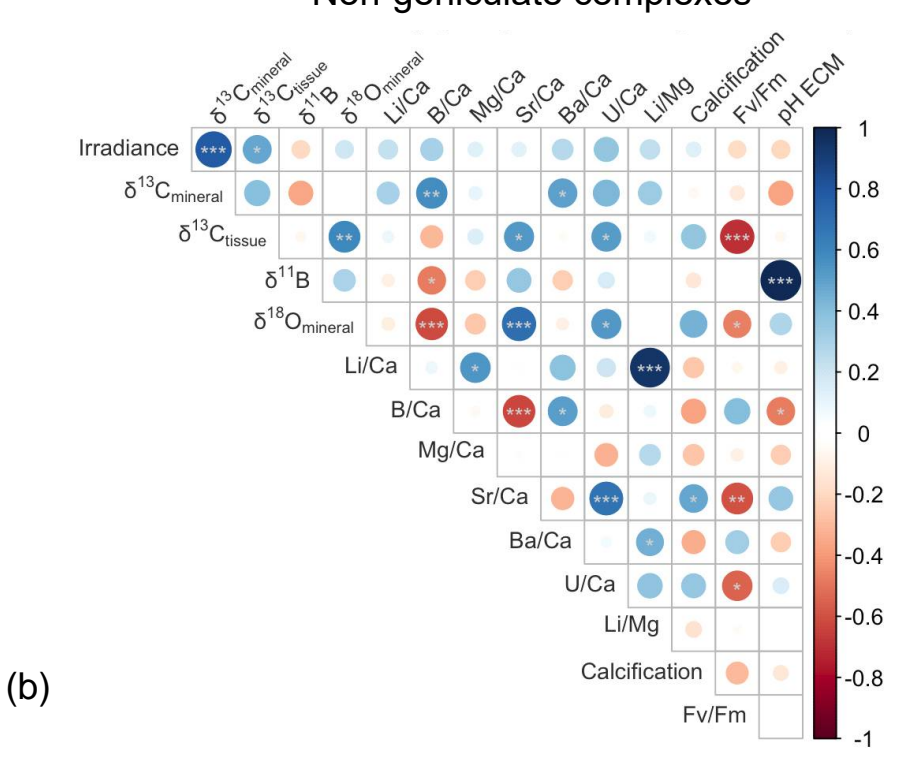


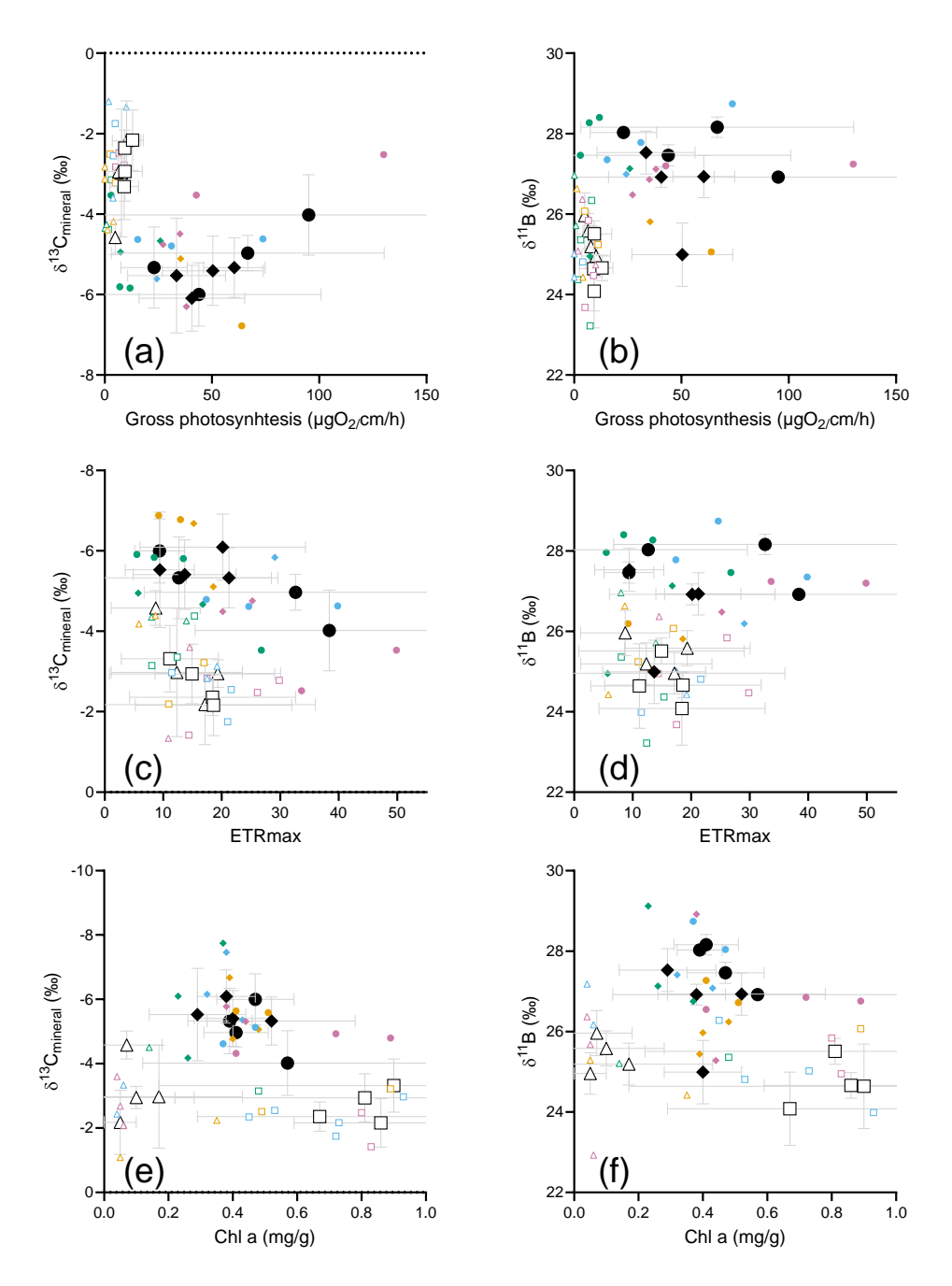
# **Correlation matrices**

## Geniculate complexes



## Non-geniculate complexes





#### Non-geniculate complexes

☐ Pneophyllum complex

Phymatolithopsis complex

#### Geniculate complexes

- Corallina/Arthrocardia "robust"
- Corallina/Arthrocardia "fine"
- Irradiance 0.6
- Irradiance 1.2
- Irradiance 1.8
- Irradiance 2.3

